กระแสวิทยาของกราฟีนสังเคราะห์ที่แขวนลอยในพอลิฟีนิลไกลซิดิลอีเทอร์โคฟอล์มาลดีไฮด์

นาย พลวัตน์ เจริญธรขจรชัย

วิทยานิพนธ์นี้เป็นส่วนหนึ่งของการศึกษาตามหลักสูตรปริญญาวิศวกรรมศาสตรมหาบัณฑิต
สาขาวิชาวิศวกรรมเคมี ภาควิชาวิศวกรรมเคมี
คณะวิศวกรรมศาสตร์ จุฬาลงกรณ์มหาวิทยาลัย
ปีการศึกษา 2554

RHEOLOGY OF SYNTHESIZED GRAPHENE SUSPENDED IN POLY[(PHENYL GLYCIDYL ETHER)-CO-FORMALDEHYDE]

Mr. Pollawat Jaroenthonkajonchai

A Thesis Submitted in Partial Fulfillment of the Requirements
for the Degree of Master of Engineering Program in Chemical Engineering
Department of Chemical Engineering
Faculty of Engineering
Chulalongkorn University
Academic Year 2011

Thesis Title	RHEOLOGY OF SYNTHESIZED GRAPHENE SUSPENDED IN POLY[(PHENYL GLYCIDYL ETHER)-CO-FORMALDEHYDE]
By	Mr. Pollawat Jaroenthonkajonchai
Field of Study	Chemical Engineering
Thesis Advisor	Assistant Professor Anongnat Somwangthanaroj, Ph.D.

Accepted by the Faculty of Engineering, Chulalongkorn University in Partial Fulfillment of the Requirements for the Master's Degree

…… Dean of the Faculty of Engineering
(Associate Professor Boonsom Lerdhirunwong, Dr.Ing.)

THESIS COMMITTEE

…… Chairman
(Associate Professor Supakanok Thongyai, Ph.D.)

…… Thesis Advisor
(Assistant Professor Anongnat Somwangthanaroj, Ph.D.)

…… Examiner
(Assistant Professor Apinan Soottitantawat, Ph.D.)

……. External Examiner
(Suttinun Phongtamrug, Ph.D.)

พลวัตน์ เจริญธรขจรชัย:กระแสวิทยาของกราฟีนสังเคราะห์ที่แขวนลอยในพอลิฟีนิลไกลซิดิลอีเทอร์โคฟอร์มาลดีไฮด์. (RHEOLOGY OF SYNTHESIZED GRAPHENE SUSPENDED IN POLY[(PHENYL GLYCIDYL ETHER)-CO-FORMALDEHYDE]) อ. ที่ปรึกษาวิทยานิพนธ์หลัก:ผศ.ดร.อนงค์นาฏ สมหวังธนโรจน์, 68 หน้า.

กราฟีนถูกสังเคราะห์จากกราไฟต์ที่มีความบริสุทธิ์สูงผ่านสองกระบวนการ คือ กระบวนการสังเคราะห์กราฟีนออกไซด์ด้วยวิธีการของฮัมเมอร์ที่ปรับปรุงแล้วและวิธีการกำจัดหมู่ออกซิเจนโดยใช้ไฮดราซีน โดยกราฟีนออกไซด์จะถูกปรับค่าความเป็นกรด-ด่างของสารแขวนลอยในน้ำให้เหมาะสมก่อน เนื่องจากกราฟีนออกไซด์ยังแขวนลอยในน้ำที่สภาวะความเป็นกลางได้ต่ำ จากการวิจัยพบว่าที่ค่าความเป็นด่างเท่ากับ12 เป็นสภาวะที่เหมาะสมที่สุด จากนั้นจึงทำการกำจัดหมู่ออกซิเจนออกโดยใช้ไฮดราซีน โดยเสถียรภาพของคอลลอยด์จะถูกวิเคราะห์ด้วยเครื่อง UV-VIS spectroscopy และวัดปริมาณประจุบนผิวของอนุภาคที่เกิดจากการปรับค่าความเป็นกรด-ด่างด้วยวิธี zeta-potential อนุภาคที่ได้ในแต่ละขั้นตอนจะถูกนำมาวิเคราะห์สมบัติทางกายภาพโดยใช้ Raman spectroscopy, SEM, TEM และ AFM ในขณะที่การวิเคราะห์หมู่ฟังก์ชั่นและสมบัติทางความร้อนของอนุภาคถูกวิเคราะห์ด้วยเครื่อง FTIR และ TG/DTA ตามลำดับ จากนั้นนำกราฟีนที่ผสมลงในอีพอกซี, พอลิฟีนิลไกลซิดิลอีเทอร์โคฟอร์มาลดีไฮด์ โดยใช้cone and plate rheometer ที่ 1-3 % โดยน้ำหนักมาวิเคราะห์สมบัติการไหลที่สภาวะ steady state และที่ 5-9 %โดยน้ำหนักของกราฟีนวิเคราะห์สมบัติการไหลจาก oscillatory measurement โดยพบว่าสมบัติการไหลสามารถอธิบายได้ด้วยโมเดลของ Casson และสมบัติความแข็งและไหลได้สามารถอธิบายได้จากวิธีของการเปลี่ยนแปลงความเครียดและการเปลี่ยนแปลงความถี่

ภาควิชา…วิศวกรรมเคมี……. ลายมือชื่อนิสิต…….....
สาขาวิชา…วิศวกรรมเคมี……. ลายมือชื่อ อ.ที่ปรึกษาวิทยานิพนธ์หลัก...……..
ปีการศึกษา……2554……..…

5370651721: MAJOR CHEMICAL ENGINEERING
KEYWORDS : GRAPHENE / EPOXY LIQUID / RHEOLOGY

POLLAWAT JAROENTHONKAJONCHAI: RHEOLOGY OF SYNTHESIZED GRAPHENE SUSPENDED IN POLY[(PHENYL GLYCIDYL ETHER)-CO-FORMALDEHYDE]. ADVISOR: ASST.PROF.ANONGNAT SOMWANGTHANAROJ,Ph.D., 68 pp.

Graphene was synthesized through two-step method. In the first step, graphene oxide (GO) was synthesized from purified graphite via modified Hummers method. Because graphene oxide poorly dispersed in aqueous solution at pH 7, the surface treatment by adjusting pH of solution for repulsive charge and homogeneous colloid solution before reducing GO with hydrazine was studied in this research. The colloidal stability of graphene oxide in aqueous solution was measured by UV-VIS spectroscopy in term of spectrum absorption and the zeta- potential technique was used for detecting surface change of particle. Then, the chemical reduction of graphene oxide to graphene sheet was done by using hydrazine hydrate. The physical properties of particle were characterized by Raman spectroscopy, SEM, TEM and AFM technique. The functional group and thermal stability of particle were characterized via FTIR, TG/DTA respectively. Graphene sheet was then mixed with epoxy, poly[(phenyl glycidyl ether)-co-formaldehyde] at 1-3 wt% loading for steady state measurement and 5-9 wt% loading for oscillatory measurement. The rheological properties of epoxy-graphene suspension were studied by cone and plate fixture. The rheological flow model was fitted in Casson model. The solid and liquid like behavior of suspension was detected from strain sweep and frequency sweep technique.

Department: Chemical Engineering Student's Signature .....
Field of Study: Chemical Engineering Advisor's Signature .....
Academic Year: 2011

ACKNOWLEDGEMENTS

I would like to express my appreciation to my advisor, Assistant Professor Dr. Anongnat Somwangthanaroj, for her kindness, great advices and encouragement me throughout the time of this research.

I am very appreciating to my chairman, Associate Professor Dr. ML. Supakanok Thongyai, Assistant Professor Dr. Apinan Soottithantawat and Dr. Suttinun Phongtamrug for great suggestion which is useful for adjusting my research.

Additionally, I would like to thank Mectec Manufacturing Corporation (Thailand) Ltd for supporting analysis and characterization equipment such as rheometer, TGA, UV-VIS and zeta-sizer. I also gratefully thank to Coax group corporation Ltd for AFM instrument support and teaching background of AFM technique. Moreover, I thank Center of excellence in particle technology for supporting instrument in this research.

Finally, I would like to thank my family for their understanding, great encouragement and willpower throughout the time of my study. Last but not least, I feel thankful to everyone who deservedly thanks for supporting, encouragement and advice me that could not be listed here.

CONTENTS

PAGE

LIST OF TABLES

TABLE **PAGE**

LIST OF FIGURES

FIGURE **PAGE**

FIGURE **PAGE**

CHAPTER I

INTRODUCTION

1.1 General Introduction

In recent years, graphene was discovered and the researchers found that graphene exhibits high electrical conductivity and thermal stability thus it is interesting material for using in several applications such as sensor and electronic devices. The structure of graphene is sp^2 carbon in hexagonal honeycomb structure bonding interlayer with Van der Waals force. Although there are several methods to synthesize graphene, the synthesized products have many structures and various numbers of layers depending on method and preparation process. Graphene oxide is the plate-like colloid when suspended in water which is less soluble at pH 7 and the stability in water is one thing researchers would like to improve. In general way for improving dispersion and stability of graphene in water is to treat charge repulsion on surface, using steric hindrance behavior from adding either polymer or surfactant and using both of their methods by polyelectrolyte. The most suitable and easy preparation method is used in this research.

Because of their excellent properties, graphene is the interesting filler in polymer. The rheological properties are the important information to study the flow properties of graphene dispersion when applied shear force which is useful for polymer composite processing. The rheology is a useful method for studying of

particle interaction and structures in suspension of colloidal particle. Graphene suspension is the colloidal system in which information in rheology is still limited thus we would like to explore it.

In this research, graphene oxide was prepared by chemical method because this method can produce high yield of products from synthesis and easy preparation. The pH of solution was then adjusted to obtain repulsive surface charge. Graphene oxide (GO) was reduced with hydrazine. After that, graphene product was mixed with epoxy, poly [(phenyl glycidyl ether)-co-formaldehyde] by sonication. Rheological properties of graphene suspended in epoxy via cone-and-plate rheometer were studied by varying concentration of graphene.

1.2 Objectives

1. To synthesize graphene from graphite via chemical method
2. To study stability of graphene oxide in aqueous suspension when varying pH
3. To obtain rheological properties of graphene suspended in poly [(phenyl glycidyl ether)-co-formaldehyde]

1.3 Scopes of the research

1. Graphene oxide is prepared from graphite by modified Hummers method.
2. Graphene is prepared from graphene oxide via chemical reduction technique with hydrazine hydrate.
3. The surface charge of graphene oxide in aqueous suspension whose zeta-potential is measured is varied by HCl and NaOH at pH 3-14.

4. Morphology, thermal stability, and chemical structure of graphene are characterized.
5. The flow behavior of 0-9 wt% graphene suspended in poly [(phenyl glycidyl ether)-co-formaldehyde] are studied by means of rheological technique (0-3 wt% for steady state and 5-9 wt% for oscillation measurement).

CHAPTER II

LITERATURE REVIEWS

2.1 Graphene

Graphene is an allotrope of carbon atom packing in a form of two dimensional hexagonal honeycomb lattices. It can be produced from hydrocarbon materials, for example, graphite, carbon nanotube and hydrocarbon gases such as methane, ethylene and benzene. Since graphene was discovered by Geim and co-workers in 2004 using scotch tape method, many investigations have been reported its excellent properties for utilizing in versatile applications. Many researchers found that graphene showed excellent electrical, thermal and mechanical properties. [1-5] Graphene is classified as a semiconductor which shows high electrical mobility (200,000 $cm^2V^{-1}s^{-1}$) and electrical conductivity is slightly higher than that of carbon nanotube. Moreover, graphene possesses superior thermal conductivity compared to carbon nanotube in which it exhibits high thermal conductivity about 4,000-5,000 $W m^{-1}K^{-1}$ at room temperature. In consideration of mechanical property, tensile strength of graphene is about 130 GPa, which is about 100 times greater than nanosteel and Young's modulus is about 1,100 GPa.

The techniques to synthesize graphene have been developed rapidly. The important factors for selection the process for graphene synthesis are high quality

(such as number of graphene layer), high quantity and easy procedure. The summary of methods, procedure of graphene synthesis and number of graphene layer in products are depicted in Table 2.1 [1, 2, 6-10]. The number of graphene layers is difficult to characterize because graphene layer is very thin. It must be measured using more than one method for comparison. In general, the thickness of graphene layer can be measured by microscopy techniques such as transmission electron microscopy (TEM) and atomic force microscopy (AFM) and it can also be identified by Raman spectroscopy.

Micromechanical cleavage or peel off method [1] produces single-layer graphene but it is hard to scale-up because of very low productivity. Although chemical vapor deposition method (CVD) [6] generates single-layer graphene, removal of graphene from metal substrate is difficult and high temperature is required. Thermal desorption of silicon or epitaxial growth method also gives single-layer graphene but expensive substrate such as 6H-SiC and 4H-SiC in high thermal process is required. Despite developing substrate with nickel thin film, the temperature in process is still higher than 700 ^{o}C. Monolayer of graphene is produced from electrochemical method [5] using graphite rod as the electrode but this method is hard to scale-up and operate in industrial scale since skillful expert is required for this technique.

Several research groups continually developed the technique to synthesize few-layer (2-10 layers) graphene. Synthesis from nanodiamond by heating graphite furnace is not appropriate because it requires very high temperature (2,200^{o}C) which is difficult for operation and scaling-up. Arc-discharge evaporation using graphite rod and electrode is quite complicated and special expert is needed for operation. In

comparison to above-mentioned synthesis methods, chemical method is chosen in this project because of low temperature process, simple for preparing equipment and easy to scale-up to industrial process. Chemical method can be divided into two main parts: conversion of graphite powder to graphene oxide and reduction of graphene oxide to graphene.

Two well-known chemical methods for conversion of graphite powder to graphene oxide (GO), in which strong oxidant is used for reaction, are Staudenmaier method and Hummers method. In Staudenmaier method, concentrated nitric and sulfuric acid is reacted with potassium chlorate to produce chlorine dioxide gas which is the toxic gas and can explode if concentration of chlorine dioxide gas is too high. Thus, Hummers method is chosen for this work. Similar to Staudenmaier method, concentrated sulfuric acid is used but oxidizing agent is changed from potassium chlorate to potassium permanganate which is much safer. [2] Graphene oxide sheet from this process is exfoliated from graphite and separated to thin layers. After oxidation, graphene oxide sheet consists of epoxide and hydroxyl group on basal plane, as well as carbonyl and carboxyl group at the edge of sheet as shown in Figure 2.1.

Table 2.1 Methods of graphene synthesis

Methods	Ref	No of layers	Procedure
Micromechanical cleavage	[1]	1	Peel off graphene from highly ordered graphite by using scotch tape or adhesive tab and transfer to Si substrate
Thermal desorption or epitaxial growth	[1, 6]	1	Use 6H-SiC to insert in electron bombardment under vacuum at 100 ^{o}C, then heat up to 1250-1450 ^{o}C and cool down on Ni substrate or using Ni coat on substrate and heat up
Chemical vapor deposition (CVD)	[1, 11]	1	Flow hydrocarbon gas that dilute with Ar under H_2 through substrate which is coated by metal film at 800-1000 ^{o}C
Electrochemical modification	[5]	1	Using purified graphite rod as electrode and apply static potential in ionic liquid-water mixture
Arc-discharge evaporation	[1]	2-3	Using purified graphite rod as anode and another graphite rod as cathode and apply current under H_2 and He in water chamber
Chemical Reduction with reducing agent	[1, 7, 8]	2-6	Mixed graphite powder with concentrated acid and oxidizing agent in ice bath and then heat up to 35 ^{o}C in 2 hours, add DI water and H_2O_2 until color change to yellow brown, wash until neutral and reduced with hydrazine in reflux
Thermal exfoliation of GO	[2]	2-7	The process to synthesize GO is the same as chemical reduction but using GO putting in long quartz tube and insert to furnace for reducing oxygen functional group
Conversion of nanodiamond	[1, 9]	4-8	Insert nanodiamond powder in graphite furnace under He or vacuum at 1650-2200 ^{o}C

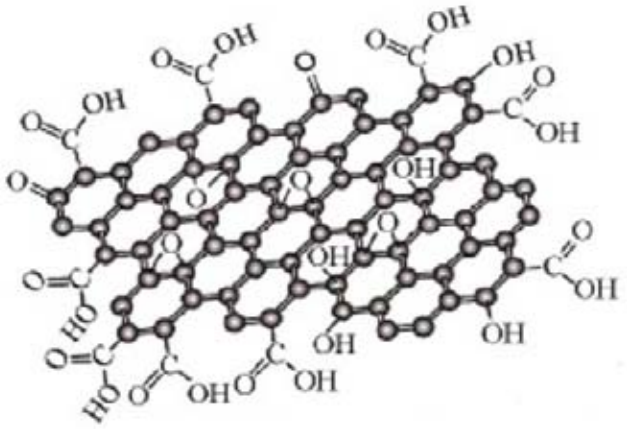

Figure 2.1 The illustration of structure of graphene oxide. [2]

The thickness of exfoliated graphene oxide sheet in aqueous suspension was measured by atomic force spectroscopy. The result was 1 nm thickness indicating that GO was slightly thicker than 0.34 nm thickness of pristine graphene sheet which might be due to the effect of covalent bond and oxygen functional group on basal plane of graphene surface [8].

However, graphene oxide can be dispersed in water or organic solvent at only small concentration and it tends to agglomerate at high concentration. Thus, it restricts the application of graphene oxide that requires high concentration. Graphene oxide suspension is the colloidal system; therefore, the stability of graphene oxide should be improved to produce well dispersion as depicted below.

2.2 Stability of graphene oxide and graphene

Graphene oxide and graphene are in the colloidal system when suspended in water and organic solvent. Although they can be dispersed in water and organic solvent better than graphite, only a small amount of them is dispersed. From this reason, many researchers have tried to find method for stabilization. In general, stability is improved by using electrostatic repulsive or surface charge method, steric hindrance from covalent linkage, combination between surface charge and steric hindrance such as polyelectrolyte and physical adsorption which are shown in Figure 2.2. [12]

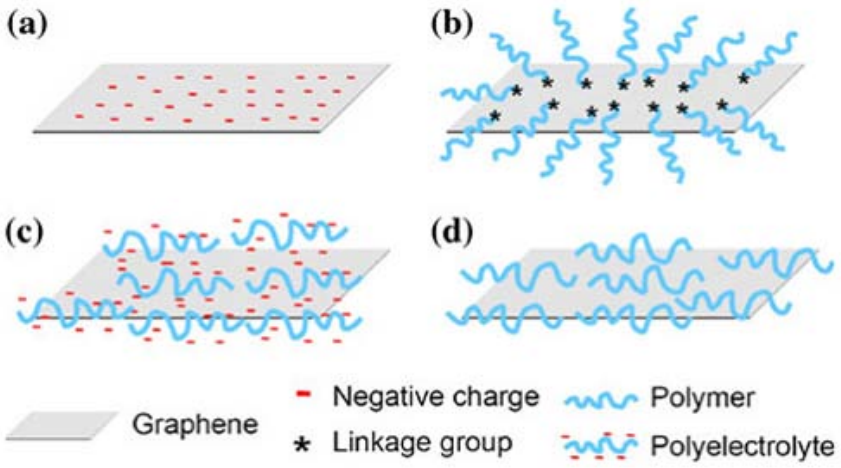

Figure 2.2 The stabilization methods of graphene in aqueous suspension a) the introduction of negative charges, b) the formation of covalent linkages, c) π-π interaction of (poly)electrolytes, and d) hydrophobic interaction of non-(poly)electrolytes. [12]

Modification of functional group by bonding covalent linkage between graphene sheet and lyophilic or conducting polymer via polymerization have been studied but this method reduced electrical conductivity of graphene sheet because of a very low electrical conductivity of lyophilic and conducting polymer. [13-15] The electrostatic repulsive of graphene and graphene oxide in aqueous suspension at various pH is the low-cost method without affecting electrical conductivity because it does not bond with polymer or surfactant. The electrostatic stability of graphene sheet depends on pH value, electrolyte concentration and concentration of particle dispersion. The graphene dispersion can be stable if the electrostatic repulsive force is greater than van der Waals force between particles.

The electrostatic stability of this system is measured by zeta-potential technique. This technique measures surface charge of particle. If there are many of surface charges of particle, the zeta-potential is far away from zero. The point of zero surface charge of particle is called isoelectric point where the particle is easy to agglomerate. The isoelectric point is the specific property of particle, for example, titania has isoelectric point around pH 5.8. The zeta-potential is the representative of surface charge potential which is measured between stern layer and diffuse layer. The surface charge value reduces exponentially until zero from particle to surface. This distance layer is called electrical double layer or Debye length. [16] Figure 2.3 shows the stern layer, diffuse layer and surface charge character of particle. If the zeta-potential is greater than + 30 or less than -30 mV, it shows the stable colloidal system. [17] From this basic colloidal system, preparation of graphene and graphene oxide in aqueous suspension using

electrostatic stabilization at various pH values is the interesting technique. For electrostatic stabilization of particle in suspension, the colloidal system is stable if the electrostatic repulsive charge is greater than van der Waals force. Although this technique was studied by using ammonia [17] and potassium hydroxide [18], there are some different conditions during synthesis. Hence, the surface charge potential in our case may be different from their researches.

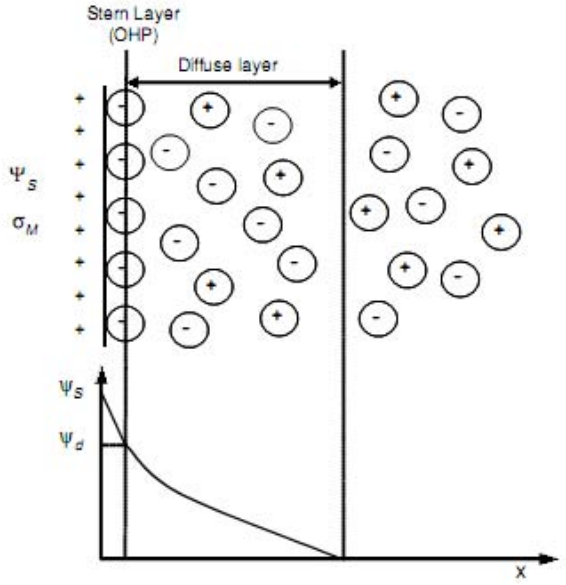

Figure 2.3 Behavior of surface charge particle via zeta-potential technique [16]

Even though oxygen functional group (carboxylic, hydroxyl, and epoxide) that occurred from conversion of graphite powder to graphene oxide process can form more stable colloidal suspension in water than graphene sheet, this oxygen functional group must be removed because it reduces electrical conductivity of pristine graphene sheet. [8, 17]

2.3 Chemical reduction of graphene oxide

There are two processes for removing oxygen on graphene oxide sheet. The first one is thermal process that is called thermal exfoliation of graphene oxide. This method begins with putting graphene oxide powder into a long quartz tube and inserting it in tube furnace which is heated up to 1,050^{o}C. The thermal process breaks the functional group of oxygen on graphene surface [1, 2]. This method must use the specifically designed equipment and high temperature. Another method is chemical reduction by using reducing agent. The commonly used reducing agent is hydrazine. Although hydrazine is a toxic substance and can be exploded if the minimum concentration reaches, it is still the best reducing agent for chemical reduction of graphene oxide to graphene at this time in comparison to other reducing agents such as ethylene glycol which is difficult to handle. [1, 8]

There are three factors that affect the process for reducing graphene via chemical reduction with hydrazine that are temperature, ratio of hydrazine to graphene oxide and time of reaction. They affect how much oxygen can be removed from graphene sheet. Graphene sheet has low oxygen on surface if high temperature, high hydrazine concentration and long reaction time are used. However, the reaction temperature is the crucial factor that must be chosen carefully and it should not be too high to avoid the explosion because hydrazine has flash point around 96^{o}C. Furthermore, the reaction must be operated in closed system under reflux condition to condense the evaporated hydrazine. Li and coworker [17] studied the influence of ratio of hydrazine to graphene oxide on electrical conductivity and they found that 7: 10 hydrazine to graphene oxide

ratio gave the electrical conductivity about 7,000 $S.m^{-1}$ and it does not change when the amount of hydrazine further increases as confirmed by elemental analysis as demonstrated in Table 2.2.

Table 2.2 Elemental analysis results of graphene prepared at various hydrazine contents [17]

$R_{N2H2/GO}$	C (wt%)	N (wt%)	H (wt%)	O (wt%)	C/N	C/O	Conductivity (S/m)
0.87:10	60.40	3.53	1.50	34.57	20.1	2.33	4
3.5:10	63.89	3.03	1.17	31.90	24.6	2.67	37
7:10	82.92	3.25	0.11	13.72	19.8	8.06	7222
35:10	85.32	3.15	0.11	11.42	31.6	9.97	7161
70:10	81.25	4.09	0.19	14.46	23.3	7.49	7272
700:10	84.25	3.78	0.40	11.57	26.0	9.71	7287

2.4 Graphene suspension in polymer solution

Selection of mixing method is a crucial factor to obtain excellent properties of composite because graphene, graphene oxide and their derivatives are difficult to disperse in polymer matrix to form suspension. There are three methods for preparing polymer composite that are physical mixing, solution blending and *in situ* polymerization. [19] The physical mixing is the method in which filler and polymer are mixed together via physical forces such as stirring, shear mixing at the molten state of polymer matrix or polymer solution. Although this process is easy and simple, filler can easily be

aggregated in matrix. The second method is the solution blending. Filler is suspended in solvent and then mixed together with polymer and solvent is then evaporated. This process improves the dispersion of filler in polymer but it is difficult to remove all solvent from composite. The last technique is *in situ* polymerization. In this method, filler is mixed with monomer or solution of monomer followed by polymerization resulting in well dispersion because monomer is inserted between the layers of filler; however, it is quite complicated. Because plate-like particle of graphene / polymer composite contains a few layers of graphene from chemical method, the composite has three states of dispersion including stacked platelet, intercalated platelet and exfoliated platelet. The morphology of polymer composite depends upon the degree of dispersion in polymer matrix. The state of plate-like particle dispersion in polymer matrix is illustrated in Figure 2.4. [19]

Because the system of graphene suspended in polymer matrix shows different rheological properties compared to that of neat polymer, the flow behavior of graphene suspension must be studied since it is an important factor to design processing condition which will be mentioned in section 2.5.

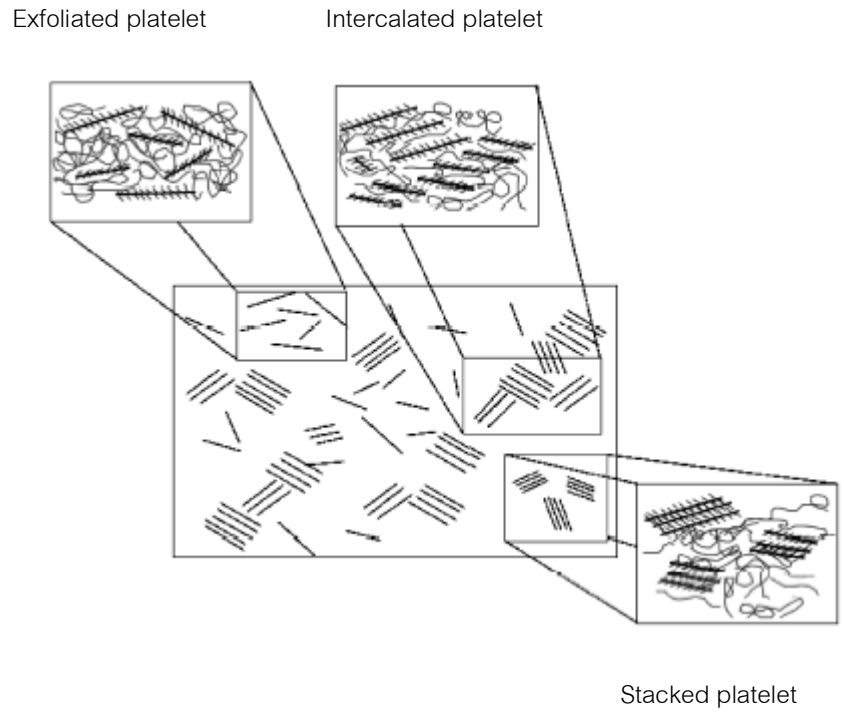

Figure 2.4 The state of plate-like particle dispersion in polymer matrix. [19]

2.5 Rheological properties of platelet particle in polymer solution

The rheological properties of particulate suspensions are sensitive to the size, size distribution, shape, surface characteristics of the dispersed phase and type of media or continuous phase. Rheology potentially offers way to assess the state of dispersion of composites in the solution. [20-22] The rheological properties can be measured in two modes: steady state and dynamic or oscillatory measurement. The steady state measurement shows the characteristic of macroscopic behavior of suspension such as flow ability, viscosity and modulus of system. The flow ability of suspension can be divided into 5 systems: Newtonian, Bingham plastic, pseudo plastic (shear thinning),

dilatants (shear t hickening) a nd shear t hinning w ith yield value.[16, 22, 23] Their rheological models are different in their flow behavior which depend on four factors that are size (size distribution) and shape o f particle, balance o f interaction force, prehistory of suspension a nd a dditional formation s uch as bridging, w hich shows c omplex rheological b ehavior.[22, 23] In general, particle suspension o ften shows shear thinning with yield value so the r eview is c onsidered only this t ype o f behavior. I n pa rticle s ize and pa rticle s ize d istribution, t he large s ize o f d iscrete ph ase exhibit high value o f viscosity but l ow y ield stress because the y ield stress depends on i nteraction between particles. T he small-sized particle has large s urface ar ea at t he s ame volume fraction when co mpared with large-sized particle. T he increasing of s urface ar ea a ffects aggregation of small s ize of particle. I t occurs easily due t o at tractive force w hich is higher than r epulsive force. Then, t he small-sized particle may be form c luster structure which means t hat t he d iscrete ph ase is d ifficult to f low. [24-27] In t erm o f size distribution e ffect, the b road size d istribution of pa rticle w ill s how lower appa rent viscosity than na rrow s ize d istribution. Bi o r multimodal s ize d istribution e xhibits lower apparent viscosity than monomodal size distribution. In this c ase, t he broad distribution and multimodal distribution of particles have much range of particle sizes in the system. The fraction of small particle prefers to stay at the vacant space between large particles and behave as a lubricant thus the viscosity and yield stress of suspension is reduced. [25-31] Regarding to the s hape o f pa rticle, t he pa rticle with high a spect r atio (L/D) o r far away from spherical shape s uch as e llipsoid, fiber, r od an d disk s hape, w ould like t o receive some extra energy dissipation or rearrange structure during flow so the viscosity

increases. [27, 28] The pre-history of suspension is another factor which affected rheological properties. Goudoulas and coworker study the effect of pre-shear time and pre-shear value. They found that the effect of pre-shear time to apparent viscosity in steady state measurement is negligible but when testing in frequency sweep measurement on viscoelastic regime, the modulus, viscosity and tan delta are shifted.[31]

The platelet particle suspension system often shows shear thinning behavior. The example of this system which is studied from other researchers is clay suspension, red blood cell system, aluminum oxide suspension and graphene suspension. [20, 21, 28, 32] Although there are many model to explain flow behavior of suspension system, most of them are extended from the general equation that is displayed in equation 2.1.[21]

$$\tau^m = \sigma_y^m + \eta_{pl}^n \dot{\gamma}^n \qquad \textbf{(2.1)}$$

In this expression, there are three functional parameters that affect flow behavior which are effective viscosity (η), shear stress (σ), and shear rate ($\dot{\gamma}$). The ultimate shear stress (σ_y) is the maximum value of system that behaves as elastic solid. It means that solid state transform to fluid state at $\sigma > \sigma_y$. At higher ultimate shear stress or yield point, the interaction of dispersed phase or interaction between dispersed phase and continuous phase is broken down thus the composite is deformed and begins to flow. The plastic viscosity (η_{pl}) is the infinite viscosity of composite which flows after deformation and destruction of aggregation from colliding of particle. It shows the equilibrium state of dispersed system after shear flow.[21-23]

. There are many model at present to explain shear thinning behavior of suspension and composite system, for example Hershell-Bulkey model, Sisko model, Bingham model, Casson model and Cross model which are displayed in equation 2.2-2.6 below.[22] The different model can be used to explain the different behavior of flow deformation and it can be used to group the material for using in the future application.

Hershell-Bulkey model: $\tau = \tau_\beta + k\dot{\gamma}^n$ (2.2)

Sisko model: $\eta = \eta_\infty + \frac{K_2}{\dot{\gamma}}$ (2.3)

Bingham model: $\tau = + \eta_{pl}\dot{\gamma}$ (2.4)

Casson model: $\tau^{1/2} = \tau_c{}^{1/2} + \eta_c{}^{1/2}\dot{\gamma}^{1/2}$ (2.5)

Cross model: $\frac{\eta - \eta(\infty)}{\eta(0) - \eta(\infty)} = \frac{1}{1 + K\dot{\gamma}^m}$ (2.6)

Another mode of rheological measurement is dynamic or oscillation measurement which can demonstrate a characteristic of microstructure or interaction between particles such as interaction force, network structure and flocculation formation. In this mode, the rheological properties can be determined from strain sweep, frequency sweep and time sweep measurement. Linear viscoelastic region can be detected from strain sweep measurement. The point where structure of suspension breaks down which can be indicated by a starting point that storage modulus (G') begins to decrease. [22, 33] Characteristic of discrete phase such as size and shape and the type of continuous phase or matrix of system are major contribution to strain in which the non-linear viscoelastic begins. If the matrix behaves as elastic material, the linear viscoelastic region is easy observed but the polymer solution system show opposite behavior. [20, 33-35] The polymer solution generally displayed viscous character so high enough content of particle or discrete phase must be added to be able to observe liner viscoelastic region of suspension system. The frequency sweep measurement gives the information regarding how composite behaves regarding elastic and viscous properties at different concentration. In this test the behavior of system depends on character of discrete phase and continuous phase. The changing behavior can be found from cross-over point where storage modulus, which is the characteristic of elastic solid, shows the same values loss modulus, which is the characteristic of viscous liquid. [33-38] The cross-over point could be found if the continuous phase has elastic solid character or dispersed phase has high concentration enough or modification of surface particle with surfactant. The surfactant affects interaction between polymer matrix and particle which may be formed network

structure. [20, 38] In the system of particle suspension in polymer solution, the cross-over point is hardly observed because polymer matrix shows viscous characteristic and at the higher concentration of particle, the system will be changed to another system from the beginning such as paste material. The time sweep measurement is the method for studying stability of polymer and polymer composite at constant stain and frequency which relates to suitable annealing time and structure of composite for using in processing. For example, Kim and coworker studied the stability of graphite and graphene in polycarbonate composite [37], whereas Wang and coworker studied the stability of organoclay in polylactic acid composite. [34]

CHAPTER III

EXPERIMENTS

3.1 Chemicals

In this research, graphite (99.99% purity, particle size≤ 45micron), hydrazine hydrate (55.1 wt%) and poly [(phenyl glycidyl ether)-co-formaldehyde] whose number range molecular weight (M_n) was about 345 g/mol, EEW = 174.8, viscosity 1595 centipoises at 52 ^{o}C were purchased from Sigma Aldrich to use as raw material, reducing agent for graphene synthesis and epoxy solution as media respectively. The other chemicals were purchased from Ajex Finechem that were sulfuric acid solution (96.3 wt%), potassium permanganate (100% purity), sodium nitrate powder (99.69% purity), sodium hydroxide pellet (99.65% purity), and hydrogen peroxide (30 vol%). Hydrochloric acid fuming (37.6 vol%) purchasing from Merck was used for washing metal ion after graphene oxide synthesis. Finally dimethylformamide (99.8% purity) purchasing from RCI labscan was used as solvent for dispersed particle.

3.2 Experimental method

3.2.1 Synthesis of graphene oxide

Graphene oxide was synthesized from graphite by modified Hummers method. 2 g of graphite powder was mixed with 50 ml of concentrated sulfuric acid and 1 g of sodium nitrate powder. After that, 6 g of potassium permanganate powder was slowly added into solution in ice bath for 1 hour and stirred on hot plate at 35 ^{o}C for 2 hours. Then 100 ml DI water was poured into the solution and it was heated up to 60 ^{o}C. Hydrogen peroxide (30 wt%) was dropped into the solution until colour was changed to yellow brown. Then, 500 ml of dilute HCl (5 vol%) was poured into it. The solution was stirred and washed with DI water several times until neutral and freeze-dried for collecting powder. The over view process can be seen in chart below.

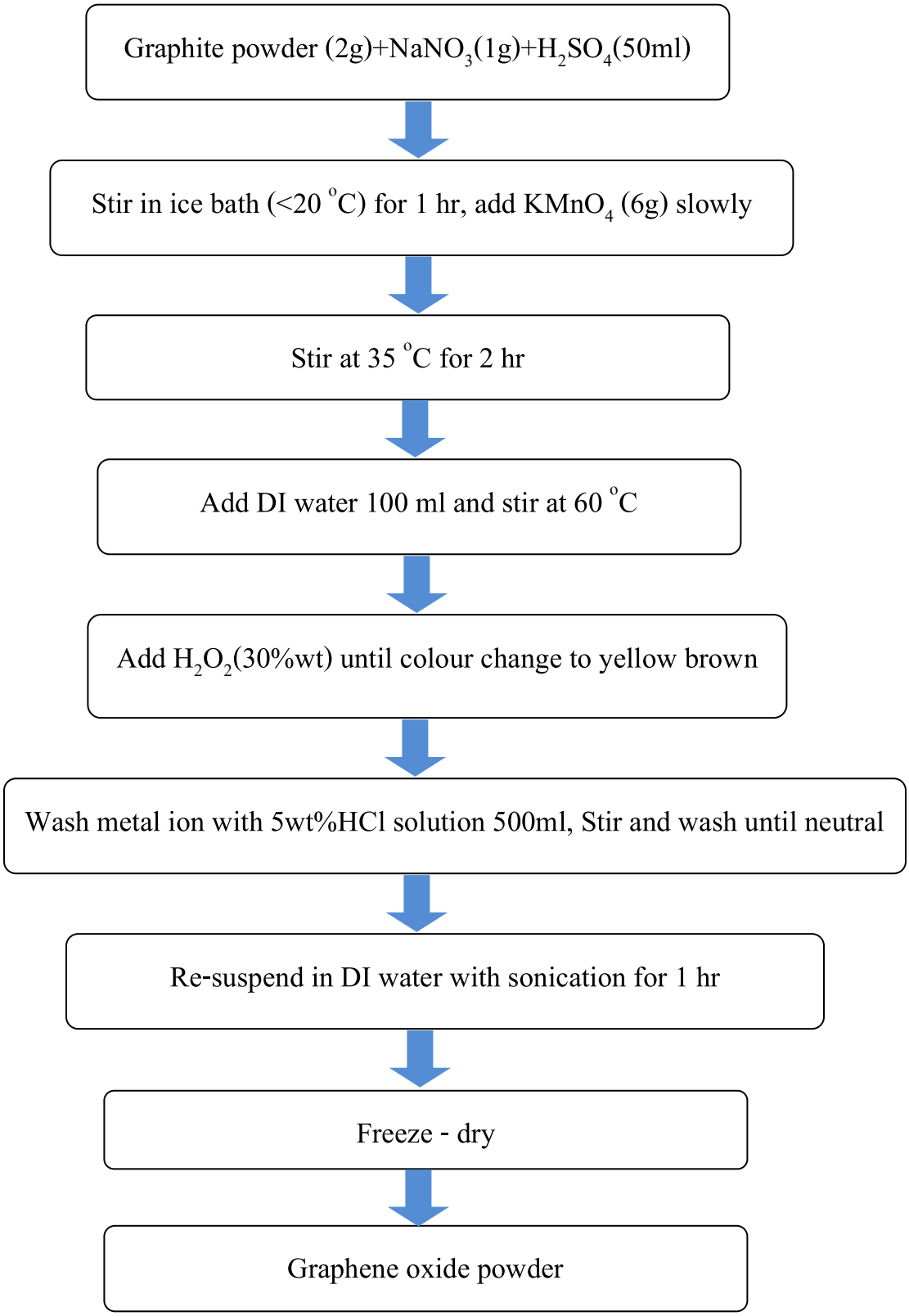
Graphite powder (2g)+$NaNO_3$(1g)+H_2SO_4(50ml)
Stir in ice bath (<20 °C) for 1 hr, add $KMnO_4$ (6g) slowly
Stir at 35 °C for 2 hr
Add DI water 100 ml and stir at 60 °C
Add H_2O_2(30%wt) until colour change to yellow brown
Wash metal ion with 5wt%HCl solution 500ml, Stir and wash until neutral
Re-suspend in DI water with sonication for 1 hr
Freeze - dry
Graphene oxide powder

3.2.2 Chemical Reduction of graphene oxide

Graphene oxide powder was re-dispersed in DI water and adjusting pH with HCl and NaOH solution. The concentration of particle in solution was 1 mg/ml. The pH of solution was adjusted until stable suspension was obtained. The solution was measured via zeta-potential technique and physical observation. The homogenous suspension was chosen to reduce graphene oxide with hydrazine hydrate (5.51 wt% in aqueous solution) at the ratio by weight of hydrazine:GO equals to 7:10. The solution in reflux system was heated-up in oil bath at 90 ^{o}C for 10 hours and it was then filtrated and washed with DI water until neutral and freeze-dried for collecting powder.

3.2.3 Sample preparation for rheological testing

Graphene was mixed in poly [(phenyl glycidyl ether)-co-formaldehyde] by magnetic stirring and sonication at 0-9 wt% of graphene. Rheological properties were studied via cone and plate rheometer. Before beginning of the test, the samples were pre-shear at 0.1 s^{-1} of shear rate; 30 sec for continuous ramp shear rate mode and pre-shear at 1 s^{-1} of shear rate; 30 sec for oscillation test.

3.3 Characterizations

3.3.1 Atomic force microscopy (AFM)

The sample powder in dimethylformamide was prepared by sonication for 30 minutes, coated on Si substrate and dried in oven overnight. After that, it was put on the stack. The sample and tip were then inserted into the microscope, aligned, adjusted maximum energy and scaned sample. The sample was tested in non-contact mode, using Nchr cantilever and collecting data with topology, non-contact mode (NCM) amplitude and non-contact mode (NCM) phase.

3.3.2 Fourier Transform Infrared Spectroscopy (FTIR)

FTIR was used to identify functional group of graphene product. It was performed in the range of 4000-650 cm^{-1}, resolution 4 cm^{-1} and identified peak in absorbance mode. The potassium bromide (KBr) was used as background material. Powder was milled with KBr and compressed by hydraulic press at 10 tons for 1 minute and put into the sample holder. The holder was placed into the sample chamber and the spectrum was recorded at least 64 scans for each spectrum.

3.3.3 Thermal Gravimetric analysis (TGA)

The degradation temperature of material was tested by TGA under nitrogen. Powder sample (7-10 mg) were loaded in ceramic pan and ramped up to 800 ^{o}C at 5 ^{o}C/min of heating rate. The N_2 gas flow rate of system was set at 50 ml/min.

3.3.4 Scanning Electron Microscopy (SEM) and Transmission Electron Microscopy (TEM)

The sample powder was dispersed in dimethylformamide and sonicated for 30 minutes, coated on Si substrate and dried in oven overnight. After that, it was put on the stack that was attached with carbon tape. It was coated with gold for conduction and put into the chamber.

3.3.5 Raman Spectroscopy

Sample powder was dried in oven overnight and pressed into the sample holder. Nd-YAG was used as the source of laser at wavelength 1064 nm. The power was applied about 50 mW and resolution of this experiment was 16 cm^{-1}.

3.3.6 Zeta sizer (Zeta-potential)

The colloidal particle in aqueous suspension (1 mg/ml) at different pH value was loaded into the cell and the cell was inserted in the chamber. After that, the electric field was applied across the particle suspension. When equilibrium was reached between two opposite charge, the velocity was measured and translated to zeta-potential value.

3.3.7 UV-VIS-NIR Spectroscopy

The colloidal particle in aqueous suspension (0.4 mg/ml) at different pH value was loaded into the cell and inserted it in the chamber. The spectrum source was applied to the sample chamber which was black body. The spectrum was scanned from 900 nm to 100 nm and the absorbance of suspension spectrum was recorded.

3.3.8 pH meter

The pH meter was calibrated with standard solution at pH4, pH7 and pH10 before using. The pH probe was washed with distillated water to remove the electrolyte that must always be soaked when it is not in use. Then, the pH probe was put into sample solution and collected the pH value from display.

3.3.9 Cone and plate rheometer

Graphene was mixed in poly[(phenyl glycidyl ether)-co-formaldehyde] at different concentration by magnetic stirring for 30 minutes followed by sonication for 45 minute. Then, it was put on the plate of rheometer and set to geometry gap (Cone angle 2^{o}, diameter 20 and 40 mm). Nitrogen gas pressure was set at 2 bars and air was set at 8 bars. The sample was pre-sheared at 0.1 s^{-1} for steady state measurement and 1 s^{-1} for oscillation measurement. The time of pre-shear was 30 second and then, rest the sample for equilibrium at 1 minute before testing the sample.

Table 3.1 Measurement and characterization of sample

Measurement	Specification	Characterizations
Atomic force microscopy (AFM)	Park system, Model : XE 100, Korea	Surface morphology, thickness of particle and particle size distribution
Fourier Transform Infrared Spectroscopy (FTIR)	Perkin Elmer instruments, Model : Spectrum GX Raman FTIR, USA	Functional group of materials
Thermal Gravimetric analysis (TGA)	Perkin Elmer instruments, Model : Diamond TG/DTA, USA	Thermal stability, Degradation temperature
Scanning Electron Microscope (SEM)	JEOL, Model : JSM-6400, Japan	Surface morphology
Transmission Electron Microscope (TEM)	JEOL, Model : JEM-2100, Japan	Surface morphology
Raman spectroscopy	Perkin Elmer instruments, Model : Spectrum GX FT-Raman , USA	Classified structure of material
Zeta sizer	Malvern, Model : ZEN 3600, UK	Surface charge of colloid particle
pH meter	Exact Instrument, Model : CT-6020A, China	pH value
UV-VIS spectroscopy	Varian, Model : Carry 5000, Austraria	Colloid stability
Cone and plate rheometer	TA Instruments, Model : AR G2, USA	Rheological properties

CHAPTER IV

RESULTS AND DISCUSSION

The experimental results from this thesis will be demonstrated and discussed dividing into three parts. The first part concentrates on characterization of particle from synthesis process which is chemical structure, thermal properties, morphology, thickness and diameter of particle. The second part explains the electrostatic stability of graphene oxide in aqueous with various pH. The third part focuses on rheological properties of graphene suspended in epoxy liquid at different concentration of particle to show flow behavior and interaction of particle suspension.

4.1 Particle characterization

4.1.1 Chemical structure analysis

Graphene oxide was synthesized from graphite by modified Hummers method. Graphene was obtained by chemical reduction of graphene oxide with hydrazine. The functional group of graphite, graphene oxide (GO) and graphene were observed by FTIR as shown in Figure 4.1. The peak around 1700, 1650 and 1250 cm^{-1} corresponds to carboxyl and carbonyl stretching of graphene oxide respectively. The epoxy peak of graphene oxide was shown at 1000 cm^{-1} and hydroxyl stretching peak was shown at 3400 cm^{-1}. FTIR spectrum would confirm that GO had epoxy, hydroxyl, carboxyl and ketone group which was described by other researcher's work.[1, 7-9] The peaks around 1600-1700 cm^{-1} and 1150 cm^{-1} of graphene were carboxyl and carbonyl group respectively. From this result, it can be confirmed that the epoxide and

hydroxyl group of graphene oxide was reduced from hydrazine in which Gao and coworker proposed mechanism of this reaction[39]. Although it has many different ways of reaction, the epoxide and hydroxyl group are reduced.

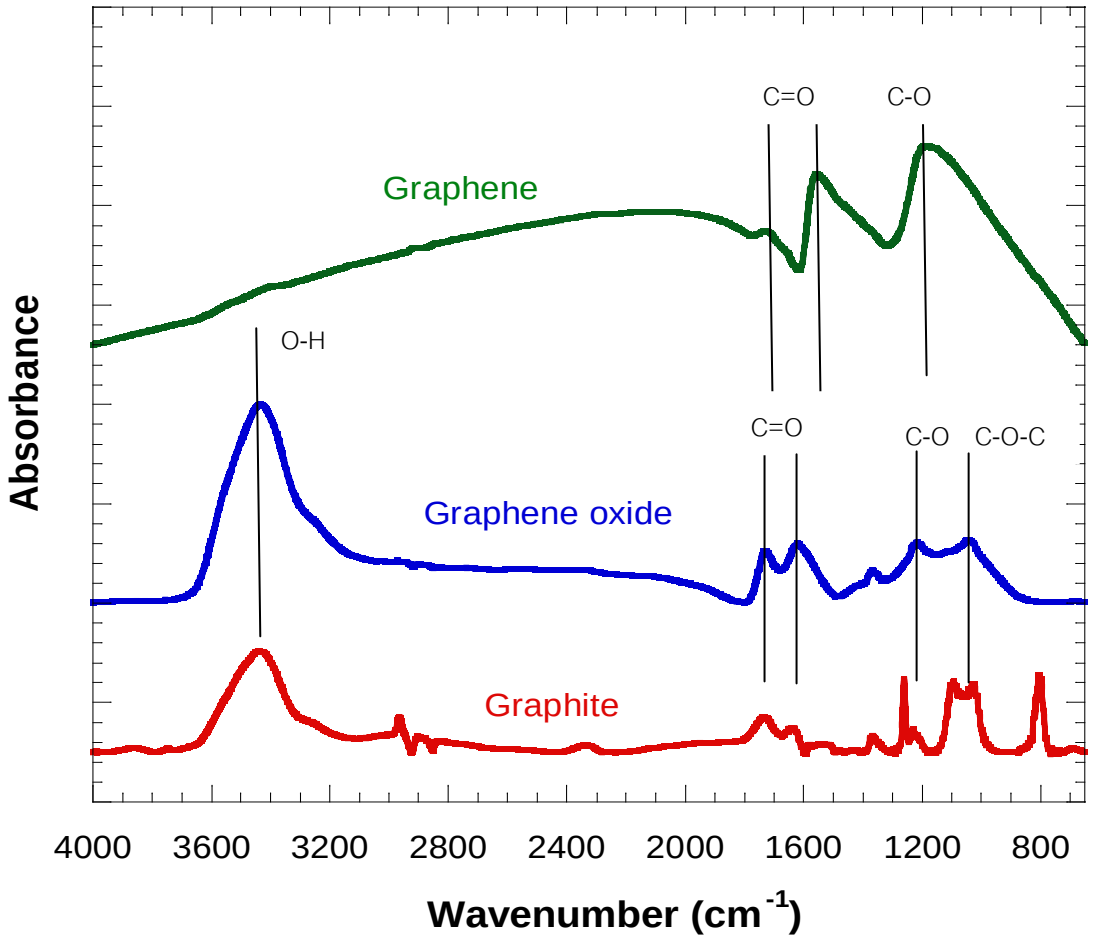

Figure 4.1 FTIR spectra of graphite, graphene oxide and graphene**.**

4.1.2 Morphology of graphene

Graphite, graphene oxide and graphene in aqueous solution were coated on Si substrate and dried in oven overnight. It was found that the size of graphene oxide and graphene were smaller than graphite because of oxidation reaction via modified Hummer method. During oxidation, graphite that consists of 100 -1000 graphene layers was separated and had the oxygen functional group on the surface which was reduced by chemical reduction with hydrazine to graphene sheet. The oxygen functional group had an effect on thermal and electrical properties of graphene. The products of synthesis were shown in Figure 4.2 in which the scale bar on SEM image of graphite, graphene oxide and graphene are 10 micrometers. The graphene product was slightly smaller size than graphene oxide particle. Because the chemical reduction just reduced oxygen functional group, it does not separate graphene sheets.

a) SEM image of Graphite

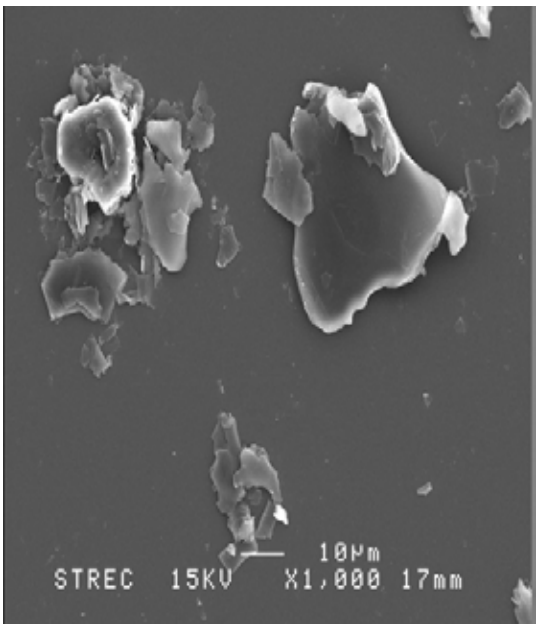

b) SEM image of Graphene oxide

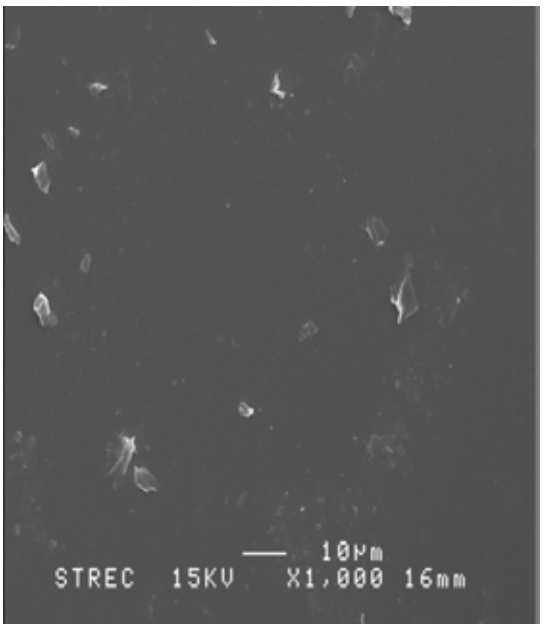

c) SEM image of Graphene

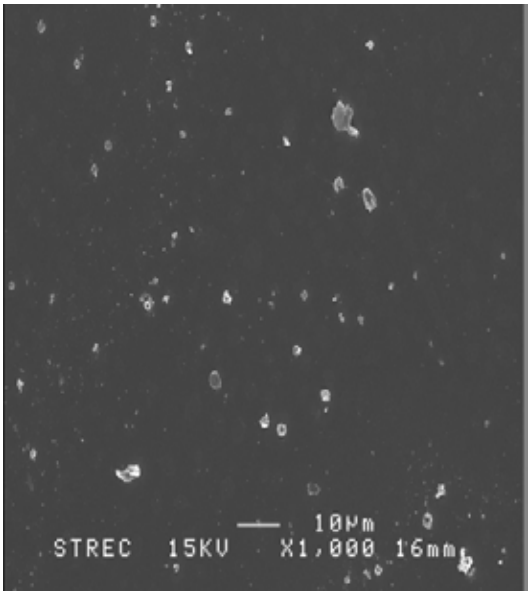

d) TEM image of Graphene

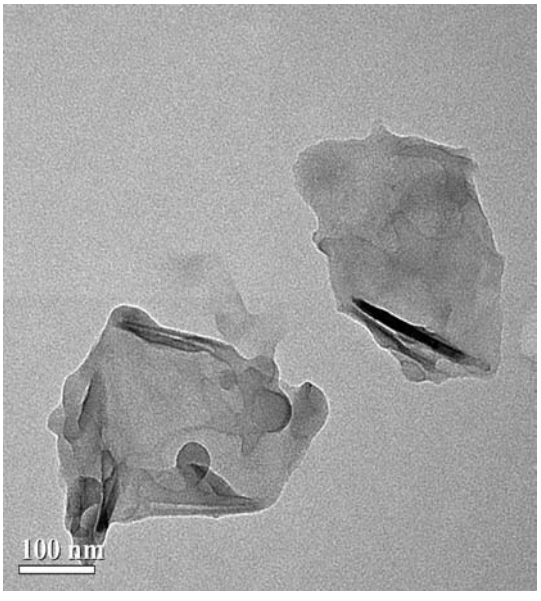

Figure 4.2 Electron microscope image of graphite, graphene oxide, graphene from SEM (a,b,c) and graphene from TEM. (d)

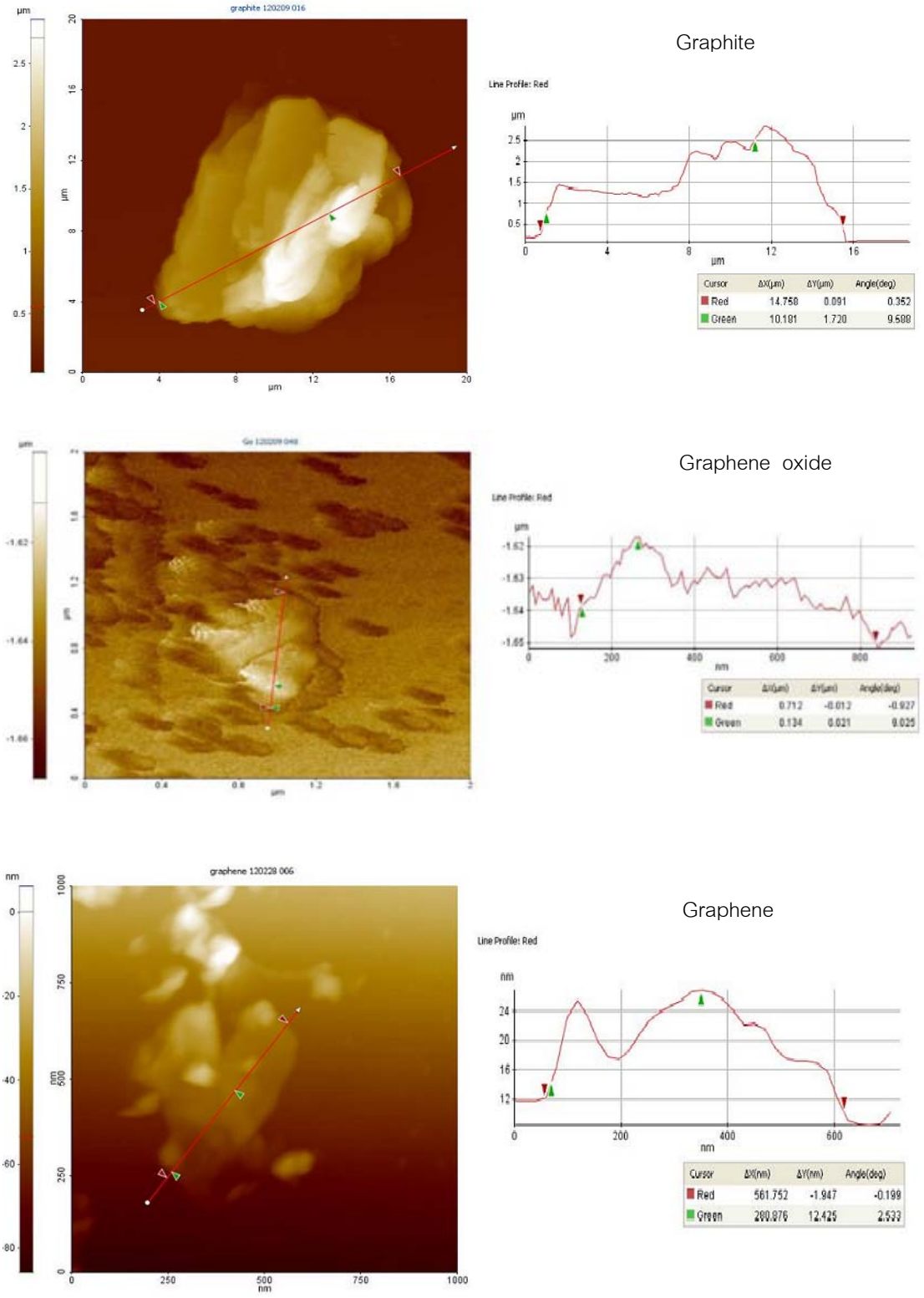

Figure 4.3 Topological image of AFM of graphite, graphene oxide and graphene respectively

Table 4.1 Result of graphite, graphene oxide and graphene from figure 4.3

Sample	Ferret's diameter (nanometer)	Thickness (nanometer)
Graphite	14,758	1,720
Graphene oxide	712	21
Graphene	561	12

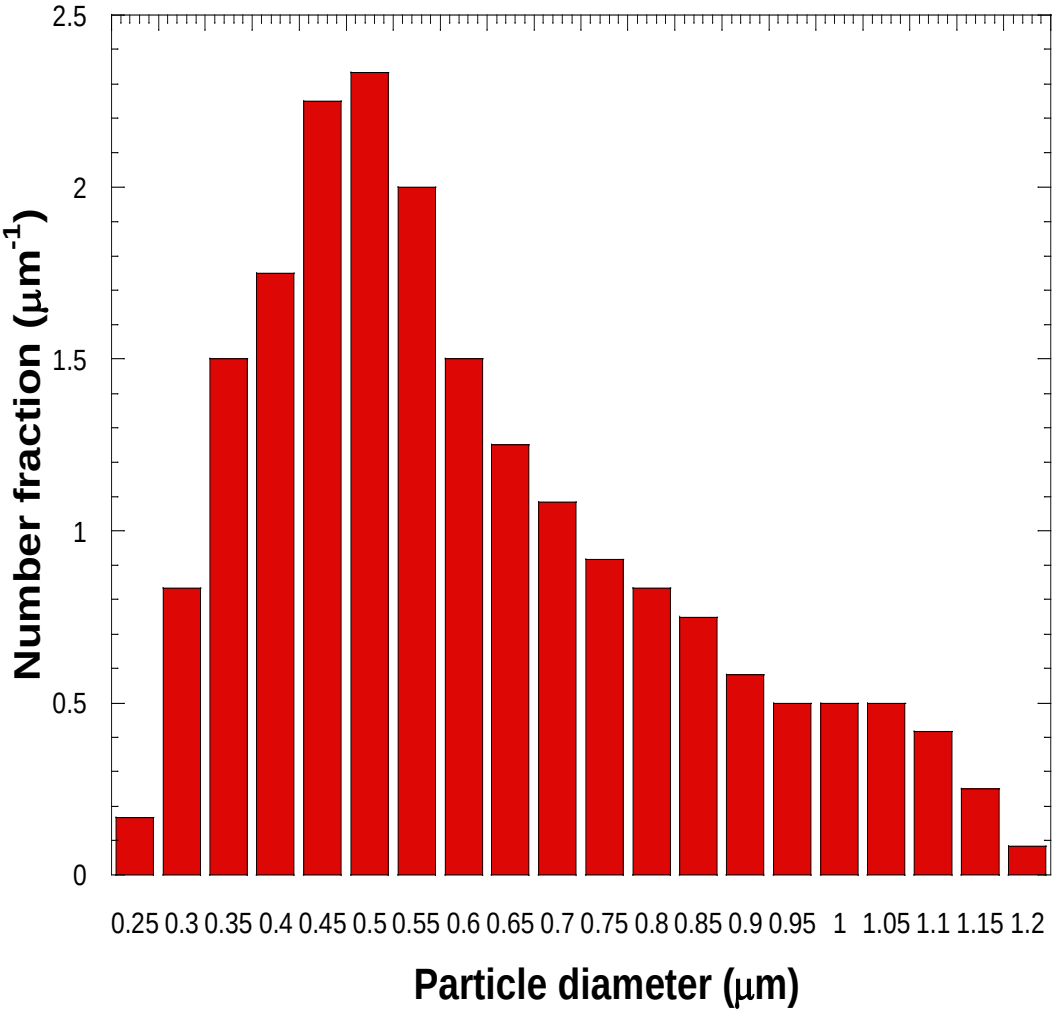

Figure 4.4 Particle size distribution of graphene product. (Data was collected from 240 particles)

The atomic force microscopy analysis can support the theory as well as the result from microscopy technique because the thickness of graphite and graphene oxide particle decrease significantly from 1.7 micrometers to 21 nanometers. The thickness of graphene is much thinner than that of graphite due to separation layer by oxidation process. In term of Ferret's diameter, graphene oxide and graphene showed significantly smaller size than graphite. Graphene is slightly smaller than graphene oxide which may be occurred from collided particle during chemical reduction process. Graphene is slightly thinner than graphene oxide which could be due to oxygen functional group reduction from hydrazine mechanism at both upper and lower plane of graphene sheet.[39] From AFM analysis, it can be estimated that the product had 10-20 layer based on thickness of carbon atom with oxygen functional group which still remains in the product.[8, 40]

Figure 4.4 showed the particle size distribution from AFM image. The size of graphene product is in the range of 0.2-1.2 micrometers. The arithmetic count mean diameter from size distribution was 0.581 micrometers. The standard deviation of this size distribution was 0.014. The particle size distribution was one factor that affects flow behavior of graphene suspension so I would like to explore it.

4.1.3 Raman spectroscopy

Raman spectra of graphite, graphene oxide and graphene were shown in Figure 4.5. Generally, Raman spectrum of carbon material was detected in G and D peak which is the bonding of sp^2 atom in both ring and chain and breathing mode of sp^2 atom in ring of carbon-carbon atom. Graphene oxide and graphene showed two intense features of G peak at about 1600 cm^{-1} and D peak at about 1300 cm^{-1} while

graphite had intensity of G peak but it was very low. Graphene oxide and graphene had intensity of G peak at 1612 and 1589 cm^{-1}. Both of graphene oxide and graphene had higher intensity of G peak than graphite because significant structure changes during chemical process.[41] It can be confirmed that graphene and graphene oxide were the structure in sp^2 carbon in hexagonal honeycomb structure. The D peak of graphene oxide and graphene are shown at 1320 and 1289 cm^{-1}. The D peak displayed the disorder or amorphous of carbon lattice.[42, 43] It was found that graphene oxide had the intensity of G peak higher than D peak but graphene showed opposite trend because of the reduction of oxygen functional group with hydrazine.[10, 44, 45] The intensity of D peak to G peak ratio of graphene oxide and graphene were 0.98 and 1.36 respectively. The in-plane crystallite size (L_a) can be calculated from intensity ratio I_D/I_G which was the characteristic of carbon material to display the electrical behavior. The in-plane crystallite size was computed from $L_a = (560/E_{laser})(I_G/I_D)$. From this relation, the in-plane crystallite size of graphene product was 220 nanometers. [9, 45, 46]

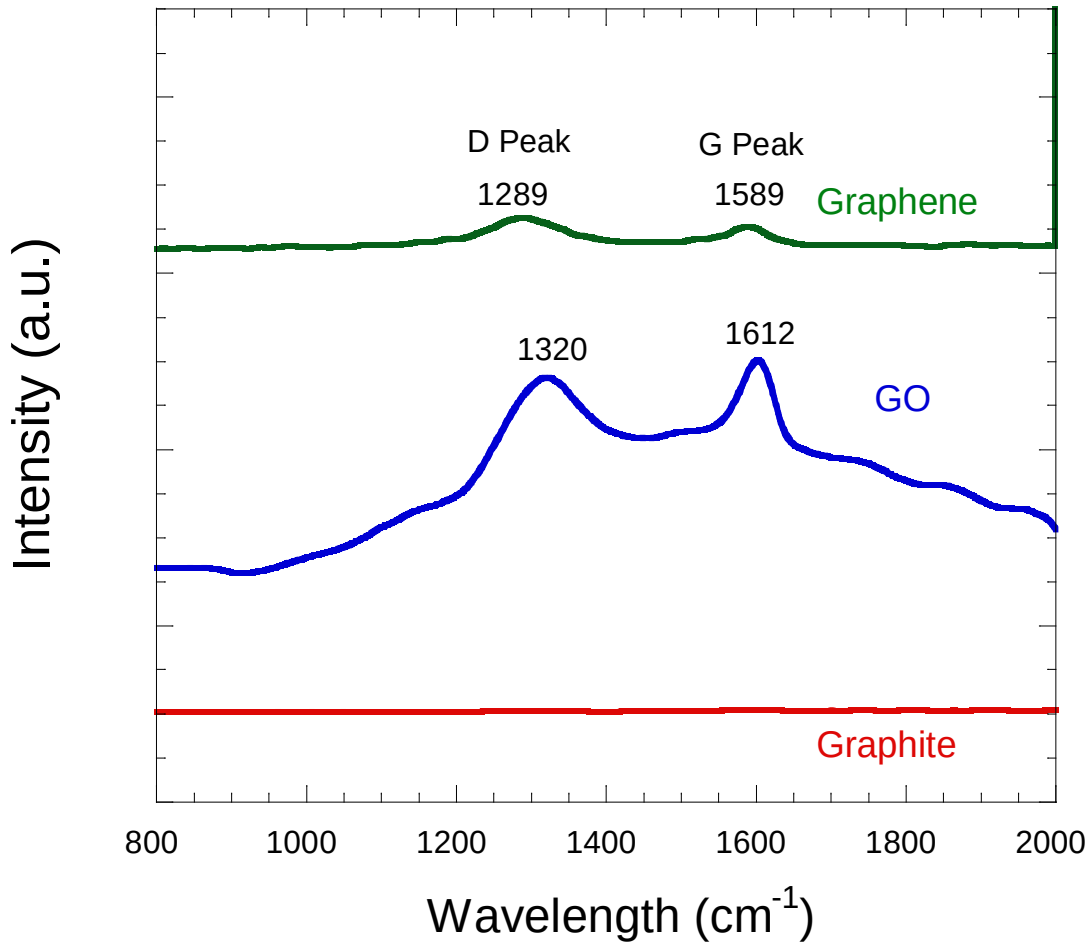

Figure 4.5 Raman spectrums of graphite, graphene oxide and graphene

4.1.4 Thermal properties of graphene

The thermal stability of graphite, graphene oxide and graphene was investigated via thermal gravimetric analysis under nitrogen atmosphere. The results were shown in Figure 4.6. Graphene oxide showed significant weight loss at 100 and 200 ^{o}C which was the evaporation of water and decomposition of oxygen containing group respectively. From the result, graphite and graphene was more thermally stable than graphene oxide but graphite was not used as filler in this research because of its large particle, less electrical and thermal conductivity.[1, 3, 37] Graphene was less

stable than graphite because of amorphous carbon structure from acid treating during graphene oxide synthesis and oxygen functional group remainder after hydrazine reduction.[13, 42, 47]

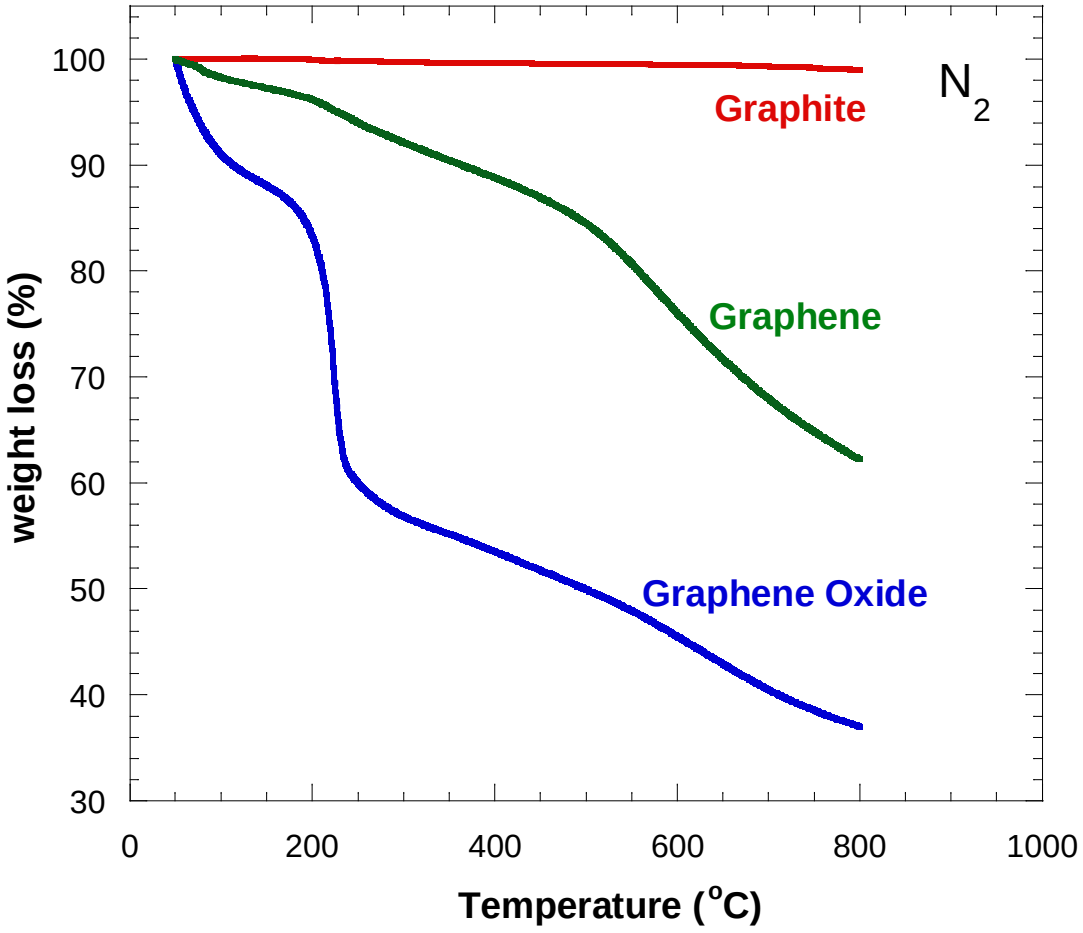

Figure 4.6 Thermal degradation of graphite, graphene oxide and graphene (Heating rate 5 °C/min)

4.2 Electrostatic stability of graphene oxide

The zeta-potential of graphene oxide (GO) in aqueous solution at 1 mg/ml was measured via nano sizer instruments at pH 3-pH 14. It was found that graphene oxide was well dispersed in aqueous solution at pH 12 and it became poorly dispersed in aqueous solution at pH higher than 12 whose physical observation are seen in Figure 4.7. The zeta-potential was reduced when the solution had higher pH and it cannot be measured at pH higher than 12 because the zeta-potential can be measured in the system with stable particle in aqueous media. The graphene oxide in suspension at pH higher than 12 precipitated so zeta-potential cannot be measured. From the result of UV-VIS spectroscopy, it was found that graphene oxide in aqueous solution was begin to absorb spectrum around 290 nanometer. The result can be divided into three groups that were the most stable graphene oxide suspension at pH 12 which showed the highest absorbance, the less stable or precipitated graphene oxide suspension (pH 13, pH 14) which showed the lowest absorption of spectrum. At pH 13 and pH 14, graphene oxide rapidly aggregated and settled down at the bottom because this condition had high amount of sodium ion and hydroxide ion which may reduce the interfacial interaction between particles and formed flocculation which affected colloid stability. [16] The last group was graphene oxide in aqueous suspension whose pH lowers than 12. This group showed lower absorbance than graphene oxide in aqueous suspension at pH 12 but higher than pH 13, pH 14 which had absorption in the range of 0.8-1.8. From above reason, it was supported that at pH 12 graphene oxide in aqueous solution shows the most stable condition from electrostatic repulsive charge method and suitable to use in the step of chemical reduction with hydrazine.

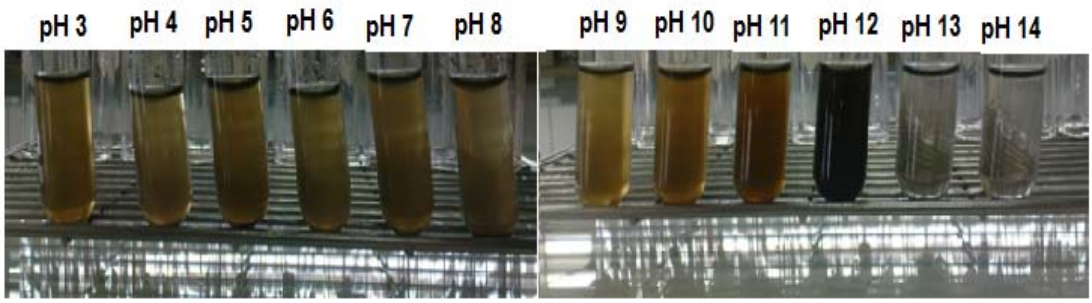

Figure 4.7 Physical observation of GO in aqueous suspension with various pH.

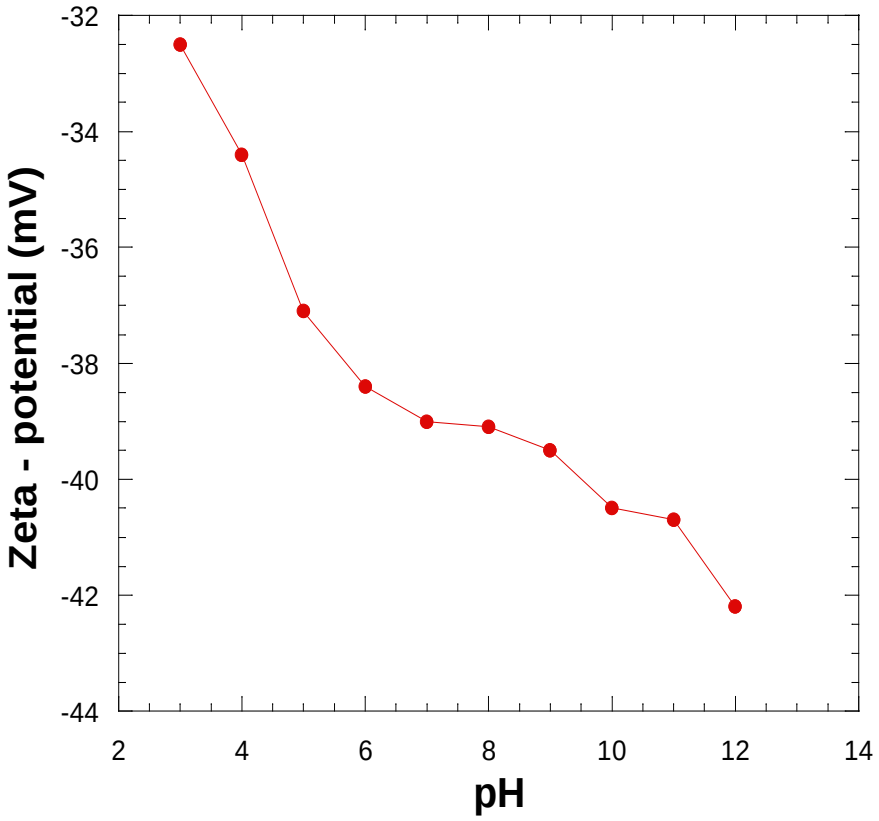

Figure 4.8 The zeta-potential of GO in aqueous suspension at pH 3-14.

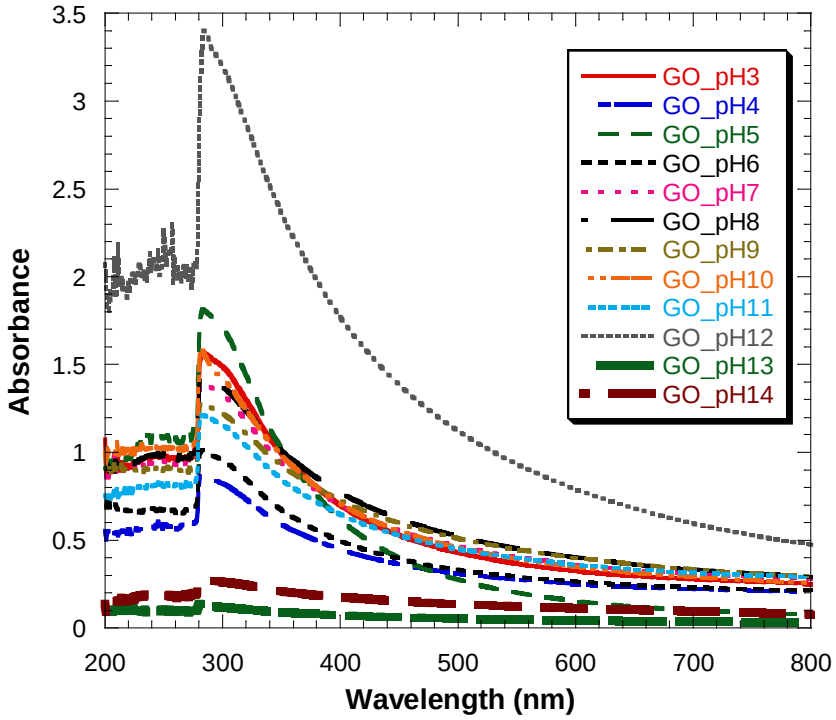

Figure 4.9 UV-VIS spectrum of graphene oxide in aqueous media at different pH value.

4.3 Rheological properties of graphene in poly [(phenyl glycidyl ether)-co-formaldehyde] media

4.3.1 Steady state measurement

The steady state measurement of rheology was studied to explain the macroscopic structure of graphene suspension in term of yield value and plastic viscosity. This test was used for exploring deformation character and processing parameter of material. In our research, graphene was mixed with poly[(phenyl glycidyl ether)-co-formaldehyde], epoxy liquid by sonication (180W, 40 kHz) for 45 minutes. The particle suspension was loaded on 25 mm, 2° cone and plate rheometer at 26 °C. The sample was pre-sheared at 0.1 s^{-1} of shear rate for 30 second and at rest

for equilibrium for 1 minute before continuous ramp of shear rate testing. The result in figure 4.10 shows Newtonian behavior for neat epoxy and become shear thinning behavior when the amount of graphene in epoxy increased. The shear thinning behavior of high graphene loading suspension showed high viscosity at low shear rate, the viscosity reduced when shear rate increased and became constant at high shear rate. The reason of this behavior was the broken of network structure between particle and media or particle interaction at the beginning thus the reduction of viscosity disappeared. When particle and network's structure was broken down to smallest size and can flow, the viscosity of suspension became constant.[22] There are many models for characterization of particle suspension that shows shear thinning behavior such as the Herschel-Bulkley General Model, the cross equation, Sisko model and Casson model [22]. When we plot between $\dot{\gamma}^{1/2}$ and $\tau^{1/2}$, it showed linear behavior which means that the graphene suspension in this epoxy fitted Casson model which can be seen in Figure 4.11.

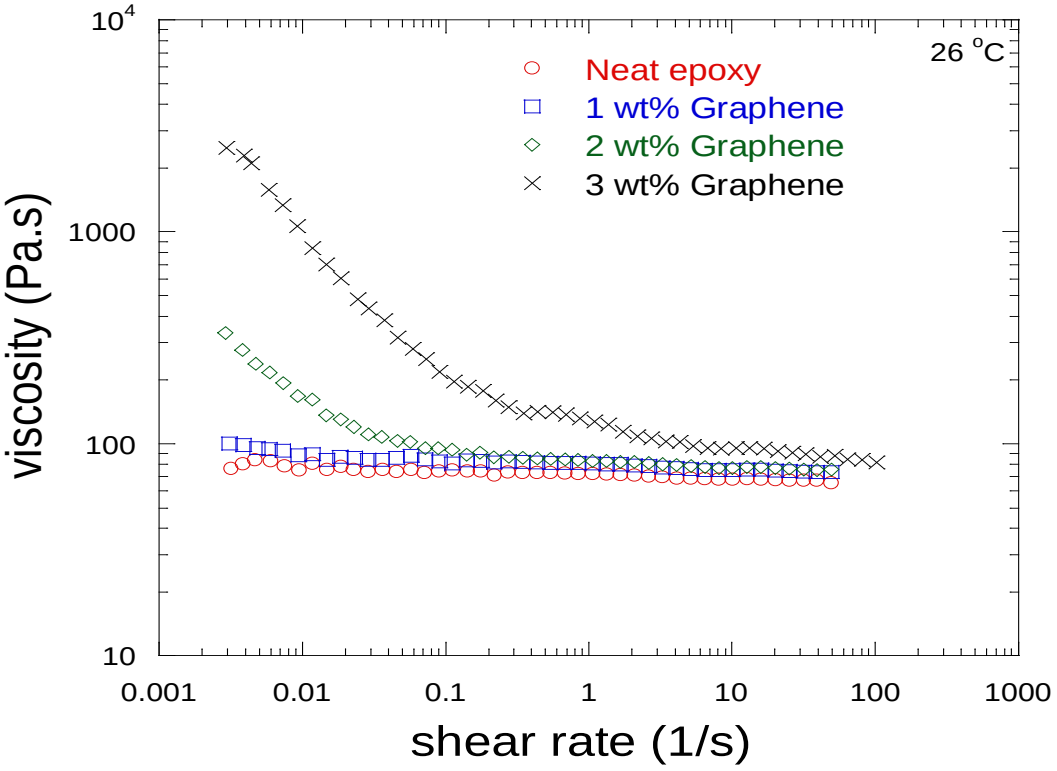

Figure 4.10 The continuous ramp shear rate of graphene suspension in poly [(phenyl glycidyl ether)-co-formaldehyde] via cone and plate (cone angle 2^{o}) rheometer.

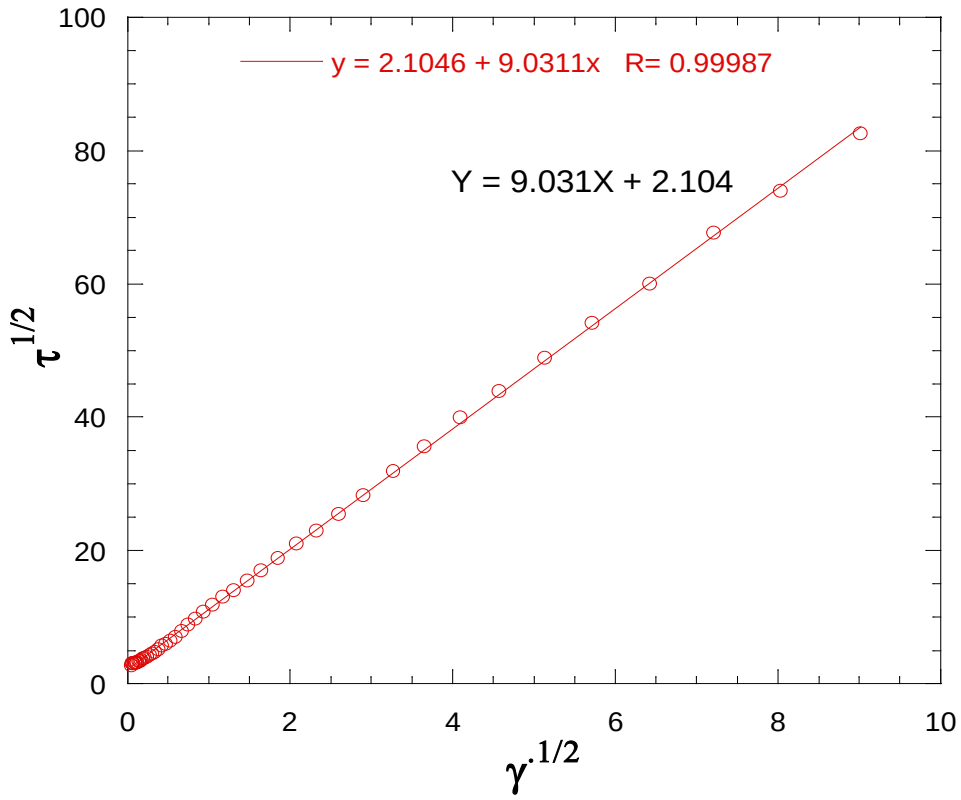

Figure 4.11 Plot between $\dot{\gamma}^{1/2}$ and $\tau^{1/2}$ from 3 wt% graphene suspension in poly [(phenyl glycidyl ether)-co-formaldehyde].

The Casson model is the flow curves use for many paints and suspension system whose equation is shown as follows

$$\tau^{1/2} = \tau_c^{1/2} + \eta_c^{1/2} \dot{\gamma}^{1/2} \qquad (4.1)$$

Where τ_c = Casson yield value

η_c = Casson plastic viscosity

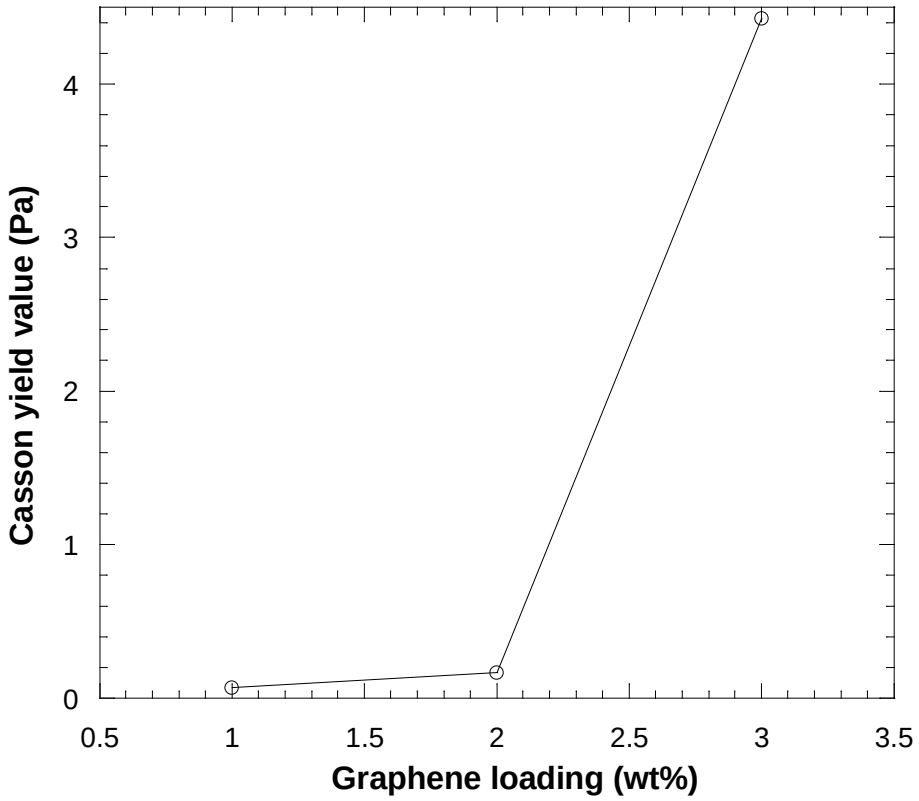

Figure 4.12 Casson yield value at different concentration of graphene suspension in poly[(phenyl glycidyl ether)-co-formaldehyde].

From equation 4.1 and graph in figure 4.11, the τ_c and η_c can be calculated from intercept and slope of graph that are 4.427 Pa and 81.559 Pa.s respectively. The Casson yield value (τ_c) is the shear stress which is used to exert the initial flow and deformation of composite. Moreover it can inform the degree of aggregation in the system. From figure 4.12, the yield value of graphene suspension at 1 and 2 wt % had significant lower than 3 wt% graphene suspension because low particle loading does not obstruct flow of suspension thus the suspension can flow easily which can be displayed from low yield stress. The Casson plastic viscosity (η_c) is a function of shear stress which must be used to maintain constant flow when aggregate of particle

was destructed to smaller size by shear force in dispersed medium.[21] It can indicate how well flow ability of composite is. From this result, it can be used to predict flow behavior of graphene in suspension system which has the same characteristic for future application.

4.3.2 Oscillation measurement

The oscillatory measurement of rheology was tested to identify microstructure of material and classified suspension material. From this mode, it can be explained how the behavior of material is, for example; how much the material shows elastic solid character and viscous liquid character. The elastic solid and viscous liquid character is the useful for processing. Moreover, the oscillation test can be used to assess the degree of dispersion of suspension in viscous media. In this research, graphene was mixed with epoxy by sonication for 45 minutes. The suspension was loaded on 40 mm, 2^{o} cone and plate rheometer at 26 ^{o}C. The sample was pre-sheared at 1 s^{-1} of shear rate for 30 second and at rest for equilibrium for 1 minute before oscillatory testing. The strain sweep measurement was used to obtain linear viscoelastic region. The linear viscoelastic region is observed when the storage modulus does not change when strain is applied.[22] It means that the storage modulus is constant with varied strain. In this region, the structure of suspension can be reconstructed to original shape when shear force is removed. Because storage modulus is the characteristic of elastic solid and the epoxy liquid showed absolutely viscous character so storage modulus of neat epoxy was hardly detected. From this reason, the storage moduli of neat epoxy and suspensions at lower than 5 wt% of graphene whose storage modulus was low and cannot see linear viscoelastic region,

were not shown in figure 4.13. It was found that at 5 wt% of graphene suspension; linear viscoelastic regime was observed from storage modulus and was shown obviously when the concentration of particle increased. However, the system with up to 9 wt% of graphene was investigated because suspension with higher than 9 wt% of graphene it became paste material which was not in scope of this work. The graphene suspension in this epoxy showed critical strain at 0.001 strains. The critical strain was the point whose storage modulus begins to decrease significantly. At this point, the structure or physical bonding of aggregated particle started to break down.[21, 22] In frequency sweep measurement, the strain was set at 0.001 and frequency was varied from 1 rad/sec to 628 rad/sec. From figure 4.14, the storage modulus of suspension increased when the particle's concentration increased. In frequency sweep test, the slopes of storage modulus at 8-9 wt % of graphene decreased when concentration of graphene increased which can be explained that the suspension showed pseudosolid-like behavior. The storage modulus of suspension increased as increasing frequency displayed more solid-like behavior at high frequency. In term of loss modulus (Figure 4.15), the results can be divided into three groups that were neat epoxy which showed the lowest value, 5 -7 wt% graphene in suspension whose value were the same behavior and 8-9 wt% graphene system whose loss moduli increased at higher concentration of particle in suspension. In the group of 8-9 wt% graphene system, the higher concentration of particle indicated higher dissipation energy because in this region graphene suspension had high concentration of particle so suspension hardly moved because particle obstructed the flow of suspension. For 5-7 wt% system, the value of loss moduli was not changed although the concentration of particle increased. It can be explained that at this condition the suspension was diluted and discrete phase

was easy to move with continuous phase thus it did not affect dissipation energy. When compared between the effect of graphene loading in term of storage modulus and loss modulus it was observed that the storage modulus increased greater than loss modulus which means that graphene loading had more effect on elastic solid character than viscous character.[48] Figure 4.16 shows the pseudosolid like behavior from frequency sweep measurement. For 8 and 9 wt% graphene system, phase angle was low at small frequency and increasing at high frequency which mean that at low frequency, 8 and 9 wt% of graphene showed higher elastic solid character than high frequency. While the phase angle of 5-7 wt% graphene system and neat epoxy was not changed with various angular frequencies. The phase angle of them was close to 90 degree which was the character of viscous material. [22, 23, 48] Finally, when plotting data between complex modulus (G*) and phase angle in figure 4.17 it was found that at 8 and 9 wt% of graphene system, the phase angle was low at small complex modulus and increasing when complex modulus increased. This behavior relates to pseudosolid-like because graphene can form network structure or agglomeration. This character can be found if concentration of particle in suspension system was high enough thus it was not observed in 5-7 wt% of graphene suspension which was dilute system. [49]

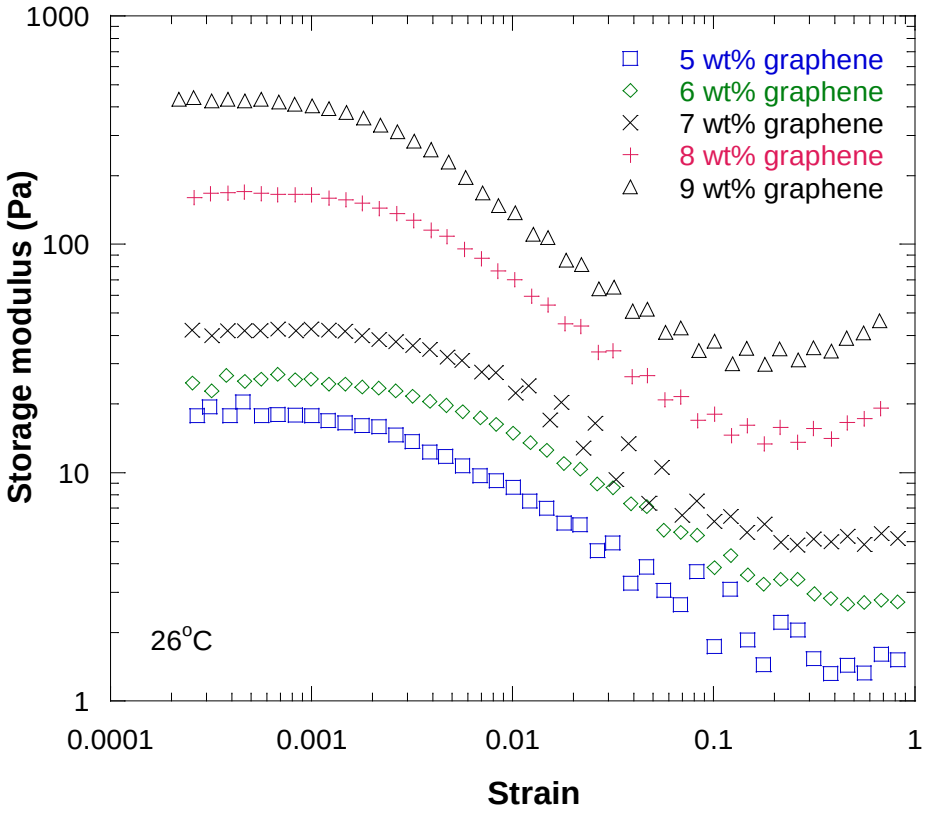

Figure 4.13 The storage modulus results of graphene suspension from stain sweep measurement. (at 1 rad/sec)

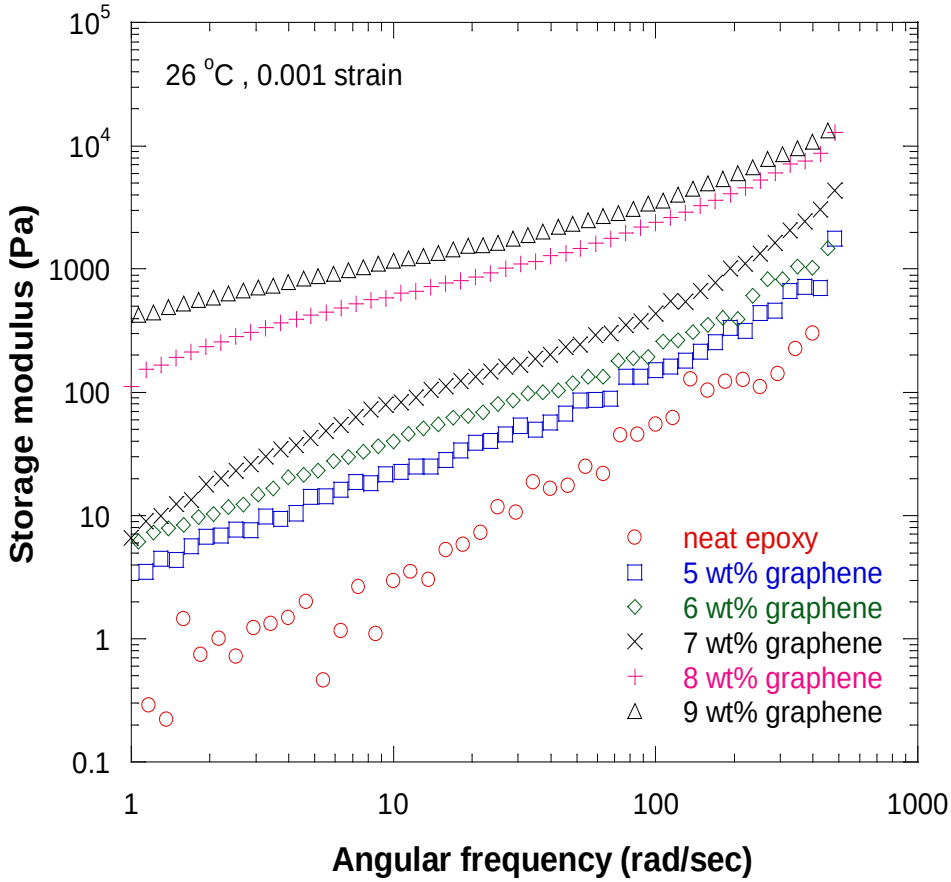

Figure 4.14 The storage modulus results of graphene suspension from frequency sweep measurement.

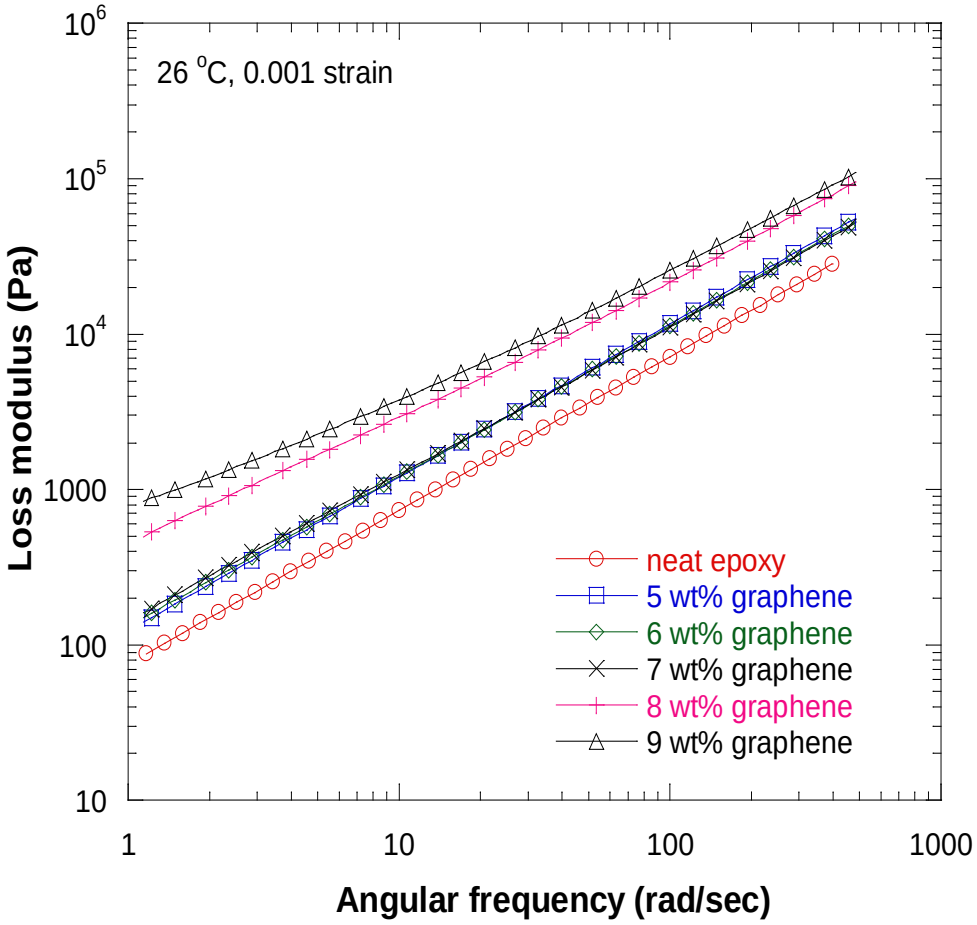

Figure 4.15 The loss modulus results of graphene suspension from frequency sweep measurement.

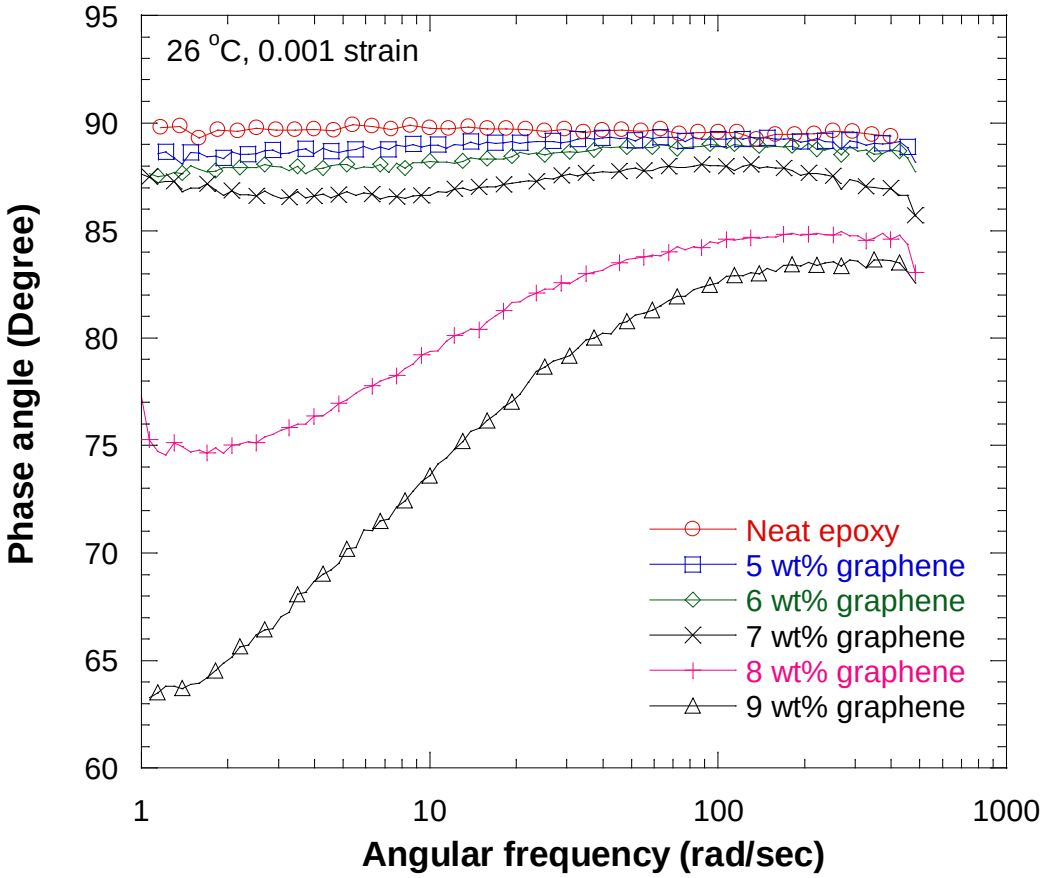

Figure 4.16 The phase angle of graphene suspension in term of angular frequency from frequency sweep measurement.

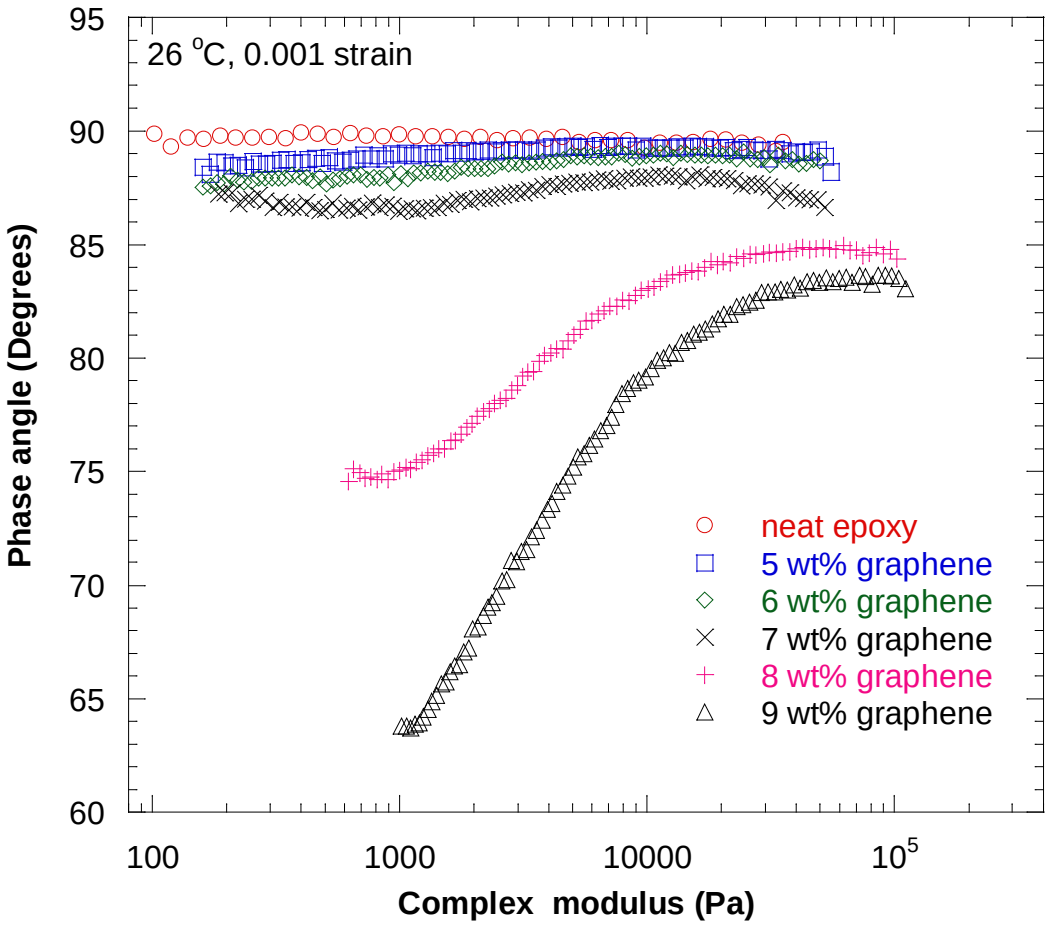

Figure 4.17 The phase angle of graphene suspension in term of complex modulus from frequency sweep measurement.

CHAPTER V

CONCLUSION AND RECOMMENDATION

5.1 Conclusion

In the first part, the particle from synthesis was characterized by FTIR, SEM, TEM, AFM, Raman spectroscopy and TGA to identify properties of graphite, graphene oxide and graphene product. It was found from chemical structure analysis that graphene product still had carboxyl and carbonyl group after chemical reduction with hydrazine. From morphology analysis, graphene oxide and graphene had the proximity size because chemical reduction did not separate graphene sheet while graphite was larger than graphene oxide due to separation sheet from oxidation process. The synthesized graphene had the arithmetic count mean diameter from particle size distribution around 581 nanometers and standard deviation around 0.014. The thickness of graphene product was 12 nanometers in which the number of layer could be around 10-20 layers based on carbon bonding of hexagonal honeycomb structure added with inter-layer spacing and some oxygen functional group remained at upper and lower planes. Then, the intensity of Raman spectrum was used to calculate in-plane crystallite size of graphene product which was about 220 nanometers. Finally, thermal stability of graphite, graphene oxide, and graphene were tested by TGA. It was observed that graphene was more thermally stable than graphene oxide because of oxygen functional group reduction but it was less stable

than graphite because oxygen functional group remainder from synthesis and amorphous carbon from acid treating during oxidation process.

In the second part, graphene oxide in aqueous suspension was analyzed in term of colloidal stability at different pH for up-scale process in the future. It was observed that at pH 12 graphene oxide showed the most stable colloidal suspension in water which was confirmed by physical observation, zeta-potential technique and UV-VIS spectroscopy.

Finally, rheological properties of graphene product was studied to explain the flow behavior of suspension and interaction of particle in poly [(phenyl glycidyl ether)-co-formaldehyde], epoxy liquid. It was observed that graphene suspended in epoxy displayed shear thinning behavior when increasing shear rate. The flow properties of this suspension can be fitted in Casson model in which the Casson yield value (τ_c = 4.427 Pa) and Casson plastic viscosity (η_c = 81.559 Pa.s) can be calculated from intercept and slope of graph between $\dot{\gamma}^{1/2}$ and $\tau^{1/2}$. The linear viscoelastic region of graphene suspended in epoxy was at strain below 0.001 and began to observe linear viscoelastic solid region from storage modulus at 5 wt% of graphene content. The physical bonding of particle-polymer or particle-particle break-down can be indicated at strain above 0.001. The linear viscoelastic properties were measured by frequency sweep from 1 rad/sec to 628 rad/sec. It was found that the storage modulus increased greater than loss modulus at the same concentration of graphene particle which means that graphene loading had more effect on storage modulus than loss modulus. The pseudosolid-like behavior showed obviously at 8-9 wt% of graphene which nearly became to paste material.

Recommendations

The synthesized step should be optimized such as reaction time at cool temperature during graphene oxide synthesis by modified Hummer method because it may affect the separation of graphene layer process and the reaction time for chemical reduction with hydrazine should be varied too because it affects oxygen content of graphene product. Moreover, the freeze-dry process after oxidation process to collect graphene oxide powder must be omitted to avoid particle agglomeration which affects thickness of graphene product. The filtration process after chemical reduction must be changed to another process for protecting the particle agglomeration via physical bonding of particle-particle interaction during filtration process.

References

[1] Rao, C.N.R., et al. A study of the synthetic methods and properties of graphenes. Science and Technology of Advanced Materials, 11(2010): 1-15.

[2] McAllister, M.J., et al. Single sheet functionalized graphene by oxidation and thermal expansion of graphite. Chemistry of Materials 19(2007): 4396-4404.

[3] Kuilla, T., et al. Recent advances in graphene based polymer composites. Progress in Polymer Science, 35(2010): 1350-1375.

[4] Park, S. and Ruoff, R.S. Chemical methods for the production of graphenes. Nature Nanotechnology, 4(2009): 217-224.

[5] Liu, N., et al. One-step ionic-liquid-assisted electrochemical synthesis of ionic-liquid-functionalized gr aphene sheets d irectly from gr aphite Advanced Functional Materials 18(2008): 1518-1525.

[6] Juang, Z.Y., et al. Synthesis of graphene on silicon carbide substrates at low temperature. Carbon, 47(2009): 2026-2031

[7] Chen, T., et al. High throughput exfoliation of graphene oxide from expanded graphite with assistance of strong oxidant in modified Hummers method. Journal of Physics: Conference Series 188(2009): 2026-2031

[8] Stankovich, S., et al. Synthesis of graphene-based nanosheets via chemical reduction of exfoliated graphite oxide. Carbon, 45(2007): 1558-1565.

[9] Subrahmanyam, K.S., Vivekchand, S.R.C., Govindaraj, A. and Rao, C.N.R. A study of graphenes prepared by different methods: Characterization, properties and solubilization. Journal of Materials Chemistry 18(2008): 1517-1523.

[10] Ferrari, A.C., et al. Raman Spectrum of graphene and graphene layers Physical Review Letters 97(2006).

[11] Sun, Z., et al. Growth of graphene from solid carbon sources Nature, 468(2010): 549-552.

[12] Yoon, S. and Insik, I. Role of poly(N-vinyl-2-pyrrolidone) as stabilizer for dispersion of graphene via hydrophobic interaction. Journal of Materials Science 46(2010): 1-6.

[13] Zhang, K., Zhang, L.L., Zhao, X.S. and Wu, J. Graphene/polyaniline nanofiber composites as supercapacitor electrodes. Chemistry of Materials 22(2010): 1392-1401.

[14] Hu, H., et al. Preparation and properties of graphene nanosheets-polystyrene nanocomposites via *in situ* emulsion polymerization. Chemical Physics Letters (484)(2010): 247-253.

[15] Wang, G., Shen, X., Wang, B., Yao, J. and Park, J. Synthesis and characterisation of hydrophilic and organophilic graphene nanosheets. Carbon, 47(2009): 1359-1364.

[16] Cosgrove, T. Colloid science - Principles, methods and applications Blackwell Publishing: UK, (2005).

[17] Li, D., Muller, M.B., Gilje, S., Kaner, R.B. and Wallace, G.G. Processable aqueous dispersions of graphene nanosheets. Nature Nanotechnology 3(2008): 101-105.

[18] Park, S., et al. Aqueous suspension and characterization of chemically modified graphene sheets Chemistry of Materials, 20(2008): 6592-6594.

[19] Solomon, M.J. and Somwangthanaroj, A. Intercalated Polypropylene Nanocomposites. Dekker Encyclopedia of Nanoscience and Nanotechnology, (2004): 1483-1490.

[20] Solomon, M.J., Almusallam, A.S., Seefeldt, K.F., Somwangthanaroj, A. and Varadan, P. Rheology of polypropylene/clay hybrid materials. Macromolecules, 34(6)(2001): 1864-1872.

[21] Matveenko, V.N. and Kirsanov, E.A. The viscosity and structure of dispersed systems. Moscow University Chemistry Bulletin, 66(4)(2011): 199-228.

[22] Tadros, T.F. Rheology of dispersions. Germany: Wiley-VCH Verlag GmbH & Co. KGaA. 2010.

[23] Larson, R.G. The stucture and rheology of complex fluids Oxford university: New York. 1999.

[24] Abdelhalim, M.A.K., Mady, M.M. and Ghannam, M.M. Rheological and dielectric properties of different gold nanoparticle sizes. Lipids in Health and Disease, 10(2011).

[25] Moelants, K.R.N., et al. Relation Between Particle Properties and Rheological Characteristics of Carrot-derived Suspensions. Food and Bioprocess Technology, (2011): 1-17.

[26] Zhang, S.S., Zhang, Y.J. and Wang, H.W. Effect of particle size distributions on the rheology of Sn/Ag/Cu lead-free solder pastes. Materials and Design, 31(1)(2010): 594-598.

[27] Genovese, D.B. Shear rheology of hard-sphere, dispersed, and aggregated suspensions, and filler-matrix composites. Advances in Colloid and Interface Science, 171-172(2012): 1-16.

[28] Calambas Pulgarin, H.L., Garrido, L.B. and Albano, M.P. Rheological properties of aqueous alumina-alumina-doped Y-PSZ suspensions. Ceramics International, 38(3)(2012): 1843-1849.

[29] He, Q., Wang, R., Wang, W., Xu, R. and Hu, B. Effect of particle size distribution of petroleum coke on the properties of petroleum coke-oil slurry. Fuel, 90(9)(2011): 2896-2901.

[30] Chun, J., Oh, T., Luna, M. and Schweiger, M. Effect of particle size distribution on slurry rheology: Nuclear waste simulant slurries. Colloids and Surfaces A: Physicochemical and Engineering Aspects, 384(1-3)(2011): 304-310.

[31] Goudoulas, T.B., Kastrinakis, E.G. and Nychas, S.G. Preparation and rheological characterization of lignite - Water slurries. Energy and Fuels, 24(1)(2010): 496-502.

[32] Korkut, S., Roy-Mayhew, J.D., Dabbs, D.M., Milius, D.L. and Aksay, I.A. High surface area tapes produced with functionalized graphene. ACS Nano, 5(6)(2011): 5214-5222.

[33] Potts, J.R., Dreyer, D.R., Bielawski, C.W. and Ruoff, R.S. Graphene-based polymer nanocomposites Polymer 52(2011).

[34] Wang, B., Wan, T. and Zeng, W. Dynamic rheology and morphology of polylactide/organic montmorillonite nanocomposites. Journal of Applied Polymer Science 121(2010): 1032-1092.

[35] Guimont, A., Beyou, E., Martin, G., Sonntag, P. and Cassagnau, P. Viscoelasticity of graphite oxide-based suspensions in PDMS Macromolecules, 44(*2011*): 3893-3900.

[36] Oh, S.M., Lee, H.I., Jeong, H.M. and Kim, B.K. The properties of functionalized graphene sheet/poly(ethyl methacrylate) nanocomposites: The effects of preparation method Macromolecular Research 19(2011): 379-384.

[37] Kim, H. and Macosko, C.W. Processing-property relationships of polycarbonate/graphene composites Polymer, 50(2009): 3797-3809.

[38] Kelarakis, A. and Giannelis, E.P. Crystallization and unusual rheological behavior in poly(ethylene oxide)-clay nanocomposites Polymer, 52(2011): 2221-2227.

[39] Gao, X., Jang, J. and Nagase, S. Hydrazine and thermal reduction of graphene oxide: Reaction mechanisms, product structures, and reaction design. Journal of Physical Chemistry C, 114(2)(2010): 832-842.

[40] Guardia, L., et al. UV light exposure of aqueous graphene oxide suspensions to promote their direct reduction, formation of graphene-metal nanoparticle hybrids and dye degradation. Carbon, 50(3)(2012): 1014-1024.

[41] Lian, P., et al. Large reversible capacity of high quality graphene sheets as an anode material for lithium-ion batteries. Electrochimica Acta, 55(12)(2010): 3909-3914.

[42] Datsyuk, V., et al. Chemical oxidation of multiwalled carbon nanotubes. Carbon, 46(6)(2008): 833-840.

[43] Musa, G., Vladoiu, R., Ciupina, V. and Janik, J. Raman spectra of carbon thin films. Journal of Optoelectronics and Advanced Materials, 8(2)(2006): 621-623.

[44] Luo, Z., et al. Electronic structures and structural evolution of hydrogenated graphene probed by Raman spectroscopy. Journal of Physical Chemistry C, 115(5)(2011): 1422-1427.

[45] Teng, C.C., et al. Thermal conductivity and structure of non-covalent functionalized graphene/epoxy composites. Carbon, 49(2011): 5107-5116.

[46] Pimenta, M.A., et al. Studying disorder in graphite-based systems by Raman spectroscopy. Physical Chemistry Chemical Physics, 9(11)(2007): 1276-1291.

[47] Hou, P., et al. Purification of single-walled carbon nanotubes synthesized by the hydrogen arc-discharge method. Journal of Materials Research, 16(9)(2001): 2526-2529.

[48] Yang, X., Zhan, Y., Zhao, R. and Liu, X. Effects of graphene nanosheets on the dielectric, mechanical, thermal properties, and rheological behaviors of poly(arylene ether nitriles). Journal of Applied Polymer Science, 124(2)(2011): 1723-1730.

[49] Huang, C.L. and Wang, C. Rheological and conductive percolation laws for syndiotactic polystyrene composites filled with carbon nanocapsules and carbon nanotubes. Carbon, 49(7)(2011): 2334-2344.

APPENDICES

Appendix A

Calculation of hydrazine to graphene oxide ratio

- Using hydrazine hydrate 5.51 wt% (dilution from 55.1 wt% in aqueous, density = 1.029 g/cm^3)
- Synthesis graphene from graphene oxide 400 mg/100 ml of solution/batch
- Ratio of hydrazine : graphene oxide = 7:10

$$\text{Using hydrazine (5.51 wt\%)} = \frac{100 \times 70 \times 4}{5.51 \times 1.029 \times 1000} = 4.938 \text{ cm}^3$$

Appendix B

Calculation of In-plane crystallite from Raman spectrum

Calculate from laser energy

- Using laser energy of Nd:YAG = 1.17 eV
- I_D/I_G of graphene spectrum was 1.356

$$L_a(nm) = \frac{560}{E_{laser}^4}\left(\frac{I_D}{I_G}\right)^{-1} \qquad (1)$$

From equation (1)

$$La\ (nm) = \frac{560}{(1.17)^4(1.356)}$$

$$= 220\ nm$$

Calculate from wave length

- Wave length of Na:YAG laser was 1064 nm

$$L_a(nm) = (2.4x10^{-10})\lambda_{laser}^4\left(\frac{I_D}{I_G}\right)^{-1} \qquad (2)$$

From equation (2)

$$La\ (nm) = \frac{(2.4x10^{-10})\ (1064)^4}{(1.356)}$$

$$= 226\ nm$$

From both equations can be calculated in-plan crystallite size about 220 nm

Appendix C

Data of particle size distribution and calculation of particle diameter

Table C.1 Data sheet of graphene particle size calculation

D_{uper}	D_{lower}	ΔD_i	D_i	n_i	f_{ni}	$f_{ni}/\Delta D_i$	C_{ni}	$f_{ni}D_i$	D_i-D_a	$(D_i$-$D_a)^2$	$f(D_i$-$D_a)^2$
0.20	0.25	0.05	0.225	2	0.008	0.167	0.008	0.002	-0.356	0.13	0.001
0.25	0.30	0.05	0.275	10	0.042	0.833	0.050	0.011	-0.306	0.09	0.004
0.30	0.35	0.05	0.325	18	0.075	1.500	0.125	0.024	-0.256	0.07	0.005
0.35	0.40	0.05	0.375	21	0.088	1.750	0.213	0.033	-0.206	0.04	0.004
0.40	0.45	0.05	0.425	27	0.113	2.250	0.325	0.048	-0.156	0.02	0.003
0.45	0.50	0.05	0.475	28	0.117	2.333	0.442	0.055	-0.106	0.01	0.001
0.50	0.55	0.05	0.525	24	0.100	2.000	0.542	0.053	-0.056	0.00	0.000
0.55	0.60	0.05	0.575	18	0.075	1.500	0.617	0.043	-0.006	0.00	0.000
0.60	0.65	0.05	0.625	15	0.063	1.250	0.679	0.039	0.044	0.00	0.000
0.65	0.70	0.05	0.675	13	0.054	1.083	0.733	0.037	0.094	0.01	0.000
0.70	0.75	0.05	0.725	11	0.046	0.917	0.779	0.033	0.144	0.02	0.001
0.75	0.80	0.05	0.775	10	0.042	0.833	0.821	0.032	0.194	0.04	0.002
0.8	0.85	0.05	0.825	9	0.038	0.750	0.858	0.031	0.244	0.06	0.002
0.85	0.90	0.05	0.875	7	0.029	0.583	0.888	0.026	0.294	0.09	0.003
0.90	0.95	0.05	0.925	6	0.025	0.500	0.913	0.023	0.344	0.12	0.003
0.95	1.00	0.05	0.975	6	0.025	0.500	0.938	0.024	0.394	0.15	0.004
1.00	1.05	0.05	1.025	6	0.025	0.500	0.963	0.026	0.444	0.20	0.005
1.05	1.10	0.05	1.075	5	0.021	0.417	0.983	0.022	0.494	0.24	0.005
1.10	1.15	0.05	1.125	3	0.013	0.250	0.996	0.014	0.544	0.30	0.004
1.15	1.20	0.05	1.175	1	0.004	0.083	1.000	0.005	0.594	0.35	0.001
				240				0.581			0.0478

Standard deviation Calculation

$$S.D. = \sqrt{\frac{\Sigma f(Di - Da)^2}{N}}$$

$$S.D. = \sqrt{\frac{0.0478}{240}} = 0.014$$

VITA

Mr. Pollawat Jaroenthonkajonchai was born in Chonburi, Thailand on April 8, 1985. He completed high school at Panuspittayakhan School, Thailand in 2004 and received the Bachelor's Degree of science from Department of Chemical Technology, Faculty of Science, Chulalongkorn University, Thailand in 2008. He entered Master's Degree in Chemical Engineering at the Department of Chemical Engineering, Faculty of Engineering, Chulalongkorn University in November, 2010.

In addition, he was invited for oral presentation in 2nd Polymer Conference of Thailand (PCT-2). His title of this presentation was rheological properties of graphene suspension in poly [(phenyl glycidyl ether)-co-formaldehyde]. This conference was held during October 20-21, 2011 at Bangkok, Thailand.